ISSN
2395-6992

International Journal of Engineering Research & Science

www.ijoer.com
www.adpublications.org

Volume-4! Issue-7! July, 2018 www.ijoer.com ! info@ijoer.com

Preface

We would like to present, with great pleasure, the inaugural volume-4, Issue-7, July 2018, of a scholarly journal, *International Journal of Engineering Research & Science*. This journal is part of the AD Publications series *in the field of Engineering, Mathematics, Physics, Chemistry and science Research Development*, and is devoted to the gamut of Engineering and Science issues, from theoretical aspects to application-dependent studies and the validation of emerging technologies.

This journal was envisioned and founded to represent the growing needs of Engineering and Science as an emerging and increasingly vital field, now widely recognized as an integral part of scientific and technical investigations. Its mission is to become a voice of the Engineering and Science community, addressing researchers and practitioners in below areas

Chemical Engineering	
Biomolecular Engineering	Materials Engineering
Molecular Engineering	Process Engineering
Corrosion Engineering	
Civil Engineering	
Environmental Engineering	Geotechnical Engineering
Structural Engineering	Mining Engineering
Transport Engineering	Water resources Engineering
Electrical Engineering	
Power System Engineering	Optical Engineering
Mechanical Engineering	
Acoustical Engineering	Manufacturing Engineering
Optomechanical Engineering	Thermal Engineering
Power plant Engineering	Energy Engineering
Sports Engineering	Vehicle Engineering
Software Engineering	
Computer-aided Engineering	Cryptographic Engineering
Teletraffic Engineering	Web Engineering
System Engineering	
Mathematics	
Arithmetic	Algebra
Number theory	Field theory and polynomials
Analysis	Combinatorics
Geometry and topology	Topology
Probability and Statistics	Computational Science
Physical Science	Operational Research
Physics	
Nuclear and particle physics	Atomic, molecular, and optical physics
Condensed matter physics	Astrophysics
Applied Physics	Modern physics
Philosophy	Core theories

Chemistry	
Analytical chemistry	Biochemistry
Inorganic chemistry	Materials chemistry
Neurochemistry	Nuclear chemistry
Organic chemistry	Physical chemistry
Other Engineering Areas	
Aerospace Engineering	Agricultural Engineering
Applied Engineering	Biomedical Engineering
Biological Engineering	Building services Engineering
Energy Engineering	Railway Engineering
Industrial Engineering	Mechatronics Engineering
Management Engineering	Military Engineering
Petroleum Engineering	Nuclear Engineering
Textile Engineering	Nano Engineering
Algorithm and Computational Complexity	Artificial Intelligence
Electronics & Communication Engineering	Image Processing
Information Retrieval	Low Power VLSI Design
Neural Networks	Plastic Engineering

Each article in this issue provides an example of a concrete industrial application or a case study of the presented methodology to amplify the impact of the contribution. We are very thankful to everybody within that community who supported the idea of creating a new Research with IJOER. We are certain that this issue will be followed by many others, reporting new developments in the Engineering and Science field. This issue would not have been possible without the great support of the Reviewer, Editorial Board members and also with our Advisory Board Members, and we would like to express our sincere thanks to all of them. We would also like to express our gratitude to the editorial staff of AD Publications, who supported us at every stage of the project. It is our hope that this fine collection of articles will be a valuable resource for *IJOER* readers and will stimulate further research into the vibrant area of Engineering and Science Research.

Mukesh Arora

(Chief Editor)

Board Members

Dr. S.R.Boselin Prabhu

Ph.D, Wireless Sensor Networks, M.E. Network Engineering, Excellent Professional Achievement Award Winner from Society of Professional Engineers Biography Included in Marquis Who's Who in the World (Academic Year 2015 and 2016). Currently Serving as Assistant Professor in the department of ECE in SVS College of Engineering, Coimbatore.

Dr. Maheshwar Shrestha

Postdoctoral Research Fellow in DEPT. OF ELE ENGG & COMP SCI, SDSU, Brookings, SD Ph.D, M.Sc. in Electrical Engineering from SOUTH DAKOTA STATE UNIVERSITY, Brookings, SD.

Zairi Ismael Rizman

Senior Lecturer, Faculty of Electrical Engineering, Universiti Teknologi MARA (UiTM) (Terengganu) Malaysia Master (Science) in Microelectronics (2005), Universiti Kebangsaan Malaysia (UKM), Malaysia. Bachelor (Hons.) and Diploma in Electrical Engineering (Communication) (2002), UiTM Shah Alam, Malaysia

Dr. D. Amaranatha Reddy

Ph.D.(Postdocteral Fellow,Pusan National University, South Korea), M.Sc., B.Sc. : Physics.

Dr. Dibya Prakash Rai

Post Doctoral Fellow (PDF), M.Sc.,B.Sc., Working as Assistant Professor in Department of Physics in Pachhuncga University College, Mizoram, India.

Dr. Pankaj Kumar Pal

Ph.D R/S, ECE Deptt., IIT-Roorkee.

Dr. P. Thangam

BE(Computer Hardware & Software), ME(CSE), PhD in Information & Communication Engineering, currently serving as Associate Professor in the Department of Computer Science and Engineering of Coimbatore Institute of Engineering and Technology.

Dr. Pradeep K. Sharma

PhD., M.Phil, M.Sc, B.Sc, in Physics, MBA in System Management, Presently working as Provost and Associate Professor & Head of Department for Physics in University of Engineering & Management, Jaipur.

Dr. R. Devi Priya

Ph.D (CSE),Anna University Chennai in 2013, M.E, B.E (CSE) from Kongu Engineering College, currently working in the Department of Computer Science and Engineering in Kongu Engineering College, Tamil Nadu, India.

Dr. Sandeep

Post-doctoral fellow, Principal Investigator, Young Scientist Scheme Project (DST-SERB), Department of Physics, Mizoram University, Aizawl Mizoram, India- 796001.

Mr. Abilash

MTech in VLSI, BTech in Electronics & Telecommunication engineering through A.M.I.E.T.E from Central Electronics Engineering Research Institute (C.E.E.R.I) Pilani, Industrial Electronics from ATI-EPI Hyderabad, IEEE course in Mechatronics, CSHAM from Birla Institute Of Professional Studies.

Mr. Varun Shukla

M.Tech in ECE from RGPV (Awarded with silver Medal By President of India), Assistant Professor, Dept. of ECE, PSIT, Kanpur.

Mr. Shrikant Harle

Presently working as a Assistant Professor in Civil Engineering field of Prof. Ram Meghe College of Engineering and Management, Amravati. He was Senior Design Engineer (Larsen & Toubro Limited, India).

Table of Contents

S.No	Title	Page No.
1	**Energy Consumption Techniques for Wireless Sensor Networks Using PSO and TSA Algorithm** **Authors:** S.Deepa, S.Kannadhasan, M.Shanmuganantham **DOI:** 10.5281/zenodo.1324100 **Digital Identification Number:** IJOER-JUL-2018-1	01-05
2	**The Use of Seismic Refraction Survey in Geotechnical Investigations** **Authors:** Bawuah, E.; Baffoe, E.; Bridget, D.; Hadir, I. A. A.; Ogbetuo, D. **DOI:** 10.5281/zenodo.1324102 **Digital Identification Number:** IJOER-JUL-2018-3	06-17
3	**Copolymerization of (p-2-Ethoxycarbonyl) cyclopropyl Styrene with Glycidyl Methacrylate** **Authors:** K.G.Guliyev, A.I.Sadygova, S.B.Mamedli, Ts.D.Gulverdashvili, A.M.Aliyeva, D.B.Tagiyev **DOI:** 10.5281/zenodo.1324104 **Digital Identification Number:** IJOER-JUL-2018-4	18-23
4	**Increase Kitchen Garden Productivity using IOT and Virtuino app** **Authors:** Prof (Dr). Jayant Shekhar, Mr. Desalegn Abebaw, Dr. Mesfin Abebe Haile **DOI:** 10.5281/zenodo.1324106 **Digital Identification Number:** IJOER-JUL-2018-5	24-28
5	**50 m-range distance and position measurement method by using two searchlights for autonomous flight device** **Authors:** Hideki Toda, Kouhei Fujiuti **DOI:** 10.5281/zenodo.1324112 **Digital Identification Number:** IJOER-JUL-2018-8	29-35

Energy Consumption Techniques for Wireless Sensor Networks Using PSO and TSA Algorithm

S.Deepa[1], S.Kannadhasan[2], M.Shanmuganantham[3]

[1]Research Scholar, Department of Computer Science, Madurai Kamaraj University, Madurai, Tamilnadu, India,
[2]Lecturer, Department of Electrical and Electronics Engineering, Tamilnadu Polytechnic College, Madurai, Tamilnadu, India.
[3]Lecturer (S.G) and Vice principal, Department of Electrical and Electronics Engineering, Tamilnadu Polytechnic College, Madurai, Tamilnadu, India.

Abstract**—** *Optimizing energy consumption is the main concern for designing and planning the operation of the Wireless Sensor Networks (WSNs). Clustering technique is one of the methods utilized to extend lifetime of the network and balancing energy consumption among sensor nodes of the network. In this paper, we propose the recently developed, heuristic optimization algorithms like Particle Swarm Optimization (PSO) and Tabu Search Algorithm(TSA) as well as the traditional Fuzzy C-Means (FCM) clustering algorithms. A comparison is made with the well known cluster-based protocol approach developed for WSNs known as harmony search algorithm which is music based Meta heuristic optimization method. Simulation results demonstrate that the proposed protocol using hybrid can reduce energy consumption and improve the network lifetime.*

Keywords**— PSO, Clustering, TSA, FCM.**

I. INTRODUCTION

In Recent developments, wireless network plays a vital role in making advance technologies in science and social welfares. Micro-electronics has created immense level of producing cheap state of network implementation in wireless technology. Advancement in the field of science has created strong base in developments of various applications such as weapons technology, life saving medical trends, agricultural fields, monitoring/predicting systems in industrial applications and process control systems. Each sensor nodes used to sense the environmental changes of the network implementation and to calculate the processed data and to communicate with the global system. It also calculates the energy levels of various networks which is an important factor to be watched out while analyzing life time of the system.

Clustering is a standard process for implementing energy efficient networks and to improvise its system performance in WSN. Each sensor nodes are grouped by various clusters based on its energy level; these clusters are processed under a cluster head detection which can process data parameters locally before being sent to a base station. LEACH and HEED network protocols provide solutions to cluster head election and to reduce energy dissipation. Testline Timing for Cluster formation Algorithm [TTCA] improves the processing time required to connect various cluster nodes both locally and globally and to maximize the network lifetime by election of proper cluster heads. It is time based chain topology which improves the performance still better compared to other network topologies.

II. CLASSIFICATION OF ALGORITHM

Clustering algorithms have created immense research oriented approaches to cover its all processes. LEACH is proposed which is the benchmark for all other processes created at later stages and provides single hop self organized clustering algorithm for wireless sensor networks. Many started developing various stages in clustering networks based on the sensing techniques, communication levels and network lifetime. It improves the transmitting range and reduces the number of nodes that communicate with the base station. It creates nodal interaction between clusters and the sink.

Energy Efficient Coverage Control Algorithm (ECCA) was proposed which is based on multi –objective genetic algorithm for full coverage of network system with improvement in lifetime. Particle Swarm Optimization [PSO is an evolution based algorithm which maintains information regarding position and velocity of each nodal structure formation.

In this paper, PSO-TS algorithm is carried out in the efficient way to improve the energy levels and to communicate the powerful link between the sensor nodes (end to end communication) with multiple constraints. It provides the basic solution for the development of improved lifetime and implements strong bondage between the structural link nodes.

In state network coverage, clustering process is carried out in sensor networks with the following assumptions:

1. All nodes remains stationary and present in the Network area are initially charged with some base energy.
2. Multi-hop situation is allowed for better communication link.
3. Nodes can be arranged randomly in the two dimensional space.
4. Constraints required for the base station from the nodes are neglected when the base station is located away from the network area.
5. GPS devices which are used to sense the network nodes are neglected.
6. Noise interference, signal fading and other losses are neglected during communication linkage.

The distance between the 'n' sensor nodes from the base station from the point P (x_i, y_i).

$$d(i, j) = (x_i - x_n)^2 + (y_i - y_n)^2 \quad [1]$$

III. PROPOSED WORK

In PSO-TS hybrid system, cluster routing is an optimal path to find the minimal cost of node selection between various clusters. If the energy present in each node is greater than the optimal energy, transmission between the nodes and communication channels are ready for sensing. The time required to analyze the structural formation of nodal networks plays a significant role in determination of time constraints. Duty cycle determines system based time constraint analysis where T_1 is the state of nodes to be active and T_2 is the state of nodes in sleep mode.

$$\textbf{Duty cycle } (\alpha) = T_1 / [T_1 + T_2] \quad [2]$$

Generation of network formation using ACO, GA, SA provides some clustering defects during analysis. This has made researchers to concentrate more in this area and to develop better solution. PSO-TS have overcome this structural defect in cluster formation with better accuracy. Nodal communication is better in test line timing approach because it provides link between the data nodes globally and locally. The intensity of pheromone and the path distance are the important factors to be considered during Ant network analysis. Ants analyze the shortest path based on the intensity of pheromone deposited in different paths.

Population based heuristic optimization algorithm which is based on food searching by birds and fish is used in Particle swarm. The population analysis is important part of network formation. Particle swarm presents an improved computation time and better cluster structure for system analysis from directional or distance based techniques.

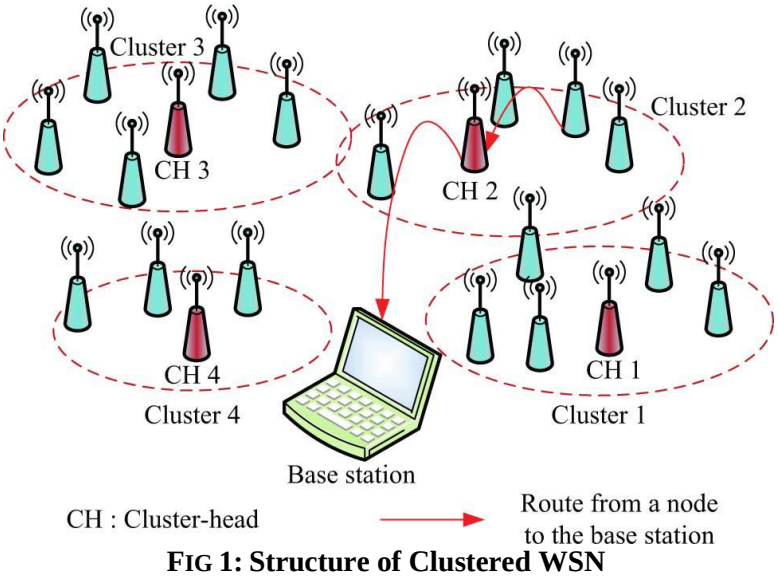

FIG 1: Structure of Clustered WSN

In PSO-TS hybrid system, many sources of system need to be analyzed and performed in each and every point of time. Energy levels are not same during each analysis of node formation. There may be collision during each process during that time energy levels may increase or decrease at certain point of time. These energy levels determine the next corresponding position of the nodal system. Cluster head detection of various sensor nodes is shown in figure.2. Network lifetime depends on the energy level consumed for each channels and the transmission between the nodes.

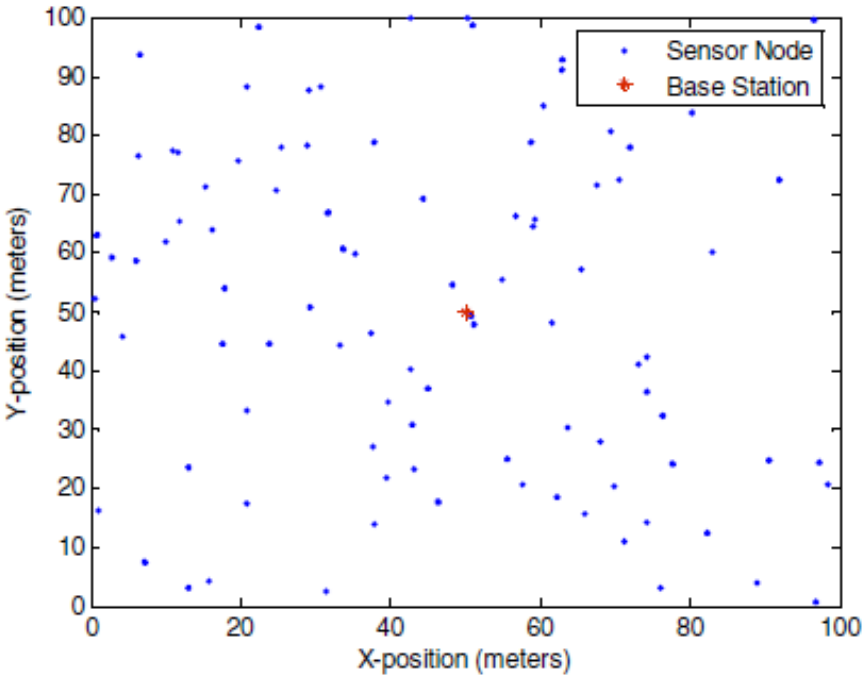

FIG 1: Cluster Head Detection from the Various Nodes

The goal is to find an appropriate initial solution for the problem, in order to get the best solution from tabu search iterations within a reasonable delay. The algorithm depicted in Fig. 1 is proposed. It starts sorting active nodes according to their degree in graph G^r decreasingly. For each iteration, the first active node i, not yet covered by the initial solution F_o, is selected. The algorithm determines the largest size clique that contains the selected active node i with adjacent nodes in graph G^r, which have yet to be covered by F_o. This clique is considered a new cluster and node i becomes the cluster head.

Algorithm does not ensure that all non active nodes are assigned to a cluster. Consequently, if node i is not covered by any cluster when the algorithm ends, it is assigned to a cluster whose head is adjacent to node i. However, this leads to the fact that an initial solution could not be feasible, i.e., a node made up of at least one cluster does not consist of a clique in the graph. A penalty equation to evaluate a solution is proposed in the following sections.

The definition of the neighbourhood Node of a solution s is a crucial step as it determines the final quality of the solution and has a direct impact on the execution time. Two types of moves are distinguished: the first move involves an ordinary node, i.e., a non active node, and the second move involves an active node. This is due to the fact that an active node could be a cluster head and thus build a new cluster. Furthermore, the third move that involves a cluster head and allows removing an existing cluster from a solution is also considered.

1. A Move Involving a Regular Node.
2. A Move Involving an Active Node.
    a. Reassigning node to a cluster whose head is adjacent to a.
    b. Select node to become the head of the cluster to which it is assigned.
3. A Move Involving a Cluster Head.

IV. SIMULATION RESULTS AND DISCUSSION

We evaluate the performance metrics for the Timeline approach for cluster formation using hybrid techniques compared with the earlier techniques. It gives enough opportunity to learn the basic techniques used in various clustering approaches. The simulation model was performed using MATLAB. We carried out basic methodology developed in LEACH for better system analysis. Our analysis focus on Generation of energy efficient cluster with respect to time and determination of network lifetime.

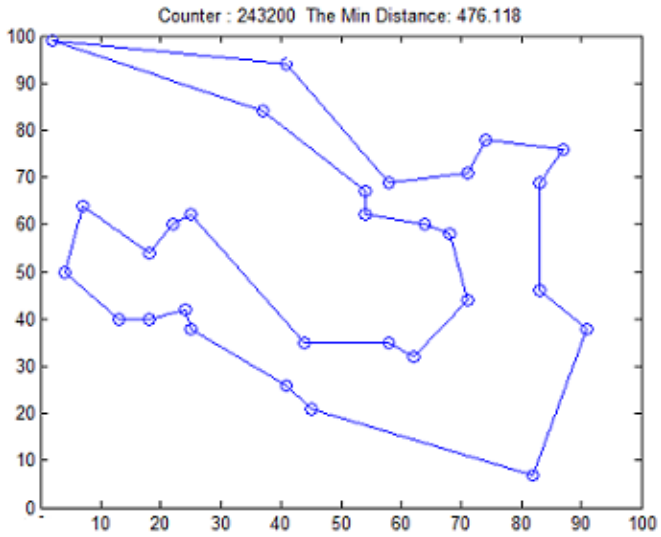

FIG:3 Simulation Result of TSA

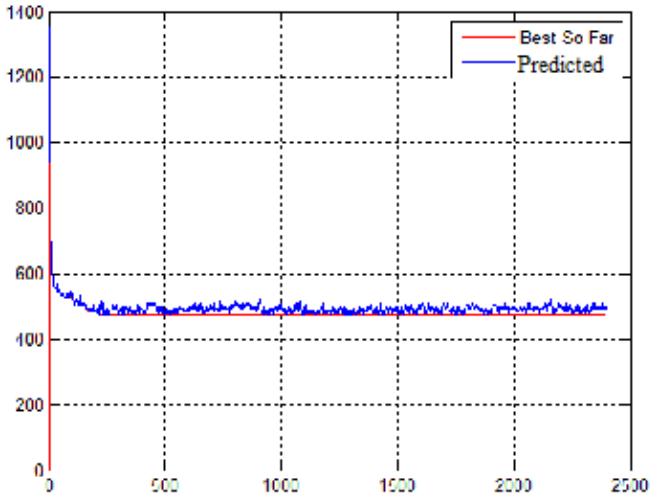

FIG 4. Simulation Result of PSO-TS

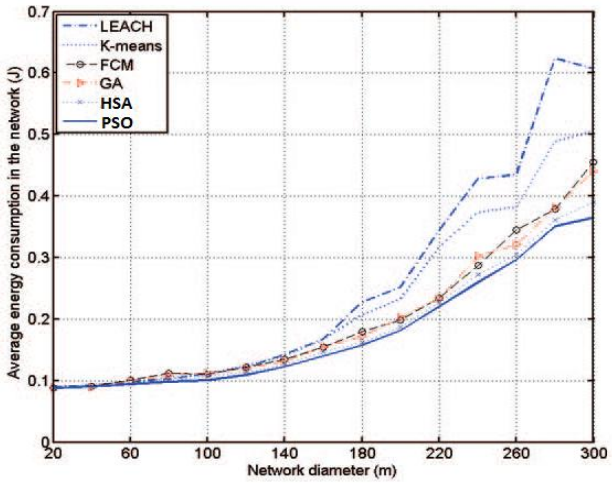

FIG 5.Comparison of Various Results

In this paper we carried out simulation for PSO-TS and compared with the earlier results of other papers. The data communications between the nodes are stronger due to better structural analysis of nodes both globally and locally. After 150 iterations, we got better results compared to LEACH and HAS algorithm. The Efficiency is improved in PSO-TS by 6 -10% more than HSA algorithm. This indicates that hybrid PSO is more stable than other optimization techniques and provides better convergence property.

V. CONCLUSION

From the analysis and simulation results, we can conclude that Hybrid optimization [PSO-TS] Algorithm used for network implementation simplifies the structural analysis between the nodes and to minimize the total energy costs which indeed extend the network lifetime considerably. PSO-TS provide higher reliability compared to other algorithms. Future works can be carried out in this field of other optimization processes such as PSO-GA, PSO-HAS.

REFERENCES

[1] Xian-hui Wang, Xuan-ping Zhang, Chun-xiao Zhuang , Zu-ning Chen, Zheng Qin, "Automatically Determining the Number of Affinity Propagation Clustering using Particle Swarm" IEEE 2010.

[2] S. Guru, S. Halgamuge, and S. Fernando, "Particle swarm optimisers for cluster formation in wireless sensor networks," in Proc. Int. Conf. Intell.Sens., Sens. Netw. Inf. Process., S. K. Halgamuge, Ed., 2005.

[3] P.K. Agarwal and C.M. Procopiuc, "Exact and Approximation Algorithms for Clustering," Algorithmica, vol. 33, no. 2, pp. 201-226, June 2002.

[4] N. M. A. Latiff, C. C. Tsimenidis, and B. S. Sharif, "Energy aware clustering for wireless sensor networks using particle swarm optimization," in Proc. 18th IEEE Int. Symp. Pers., Indoor Mobile Radio Commun., 2007.

[5] Nauman Aslam "Energy Efficient Cluster Formation Using A Multi-Criterion Optimization Technique for Wireless Sensor Networks", IEEE 2007

[6] N. Bulusu, S. Jha," Wireless Sensor Networks: A System Perspective", Artech House Inc. 2005.

[7] Ming Zou, Shijue Zheng, "A novel energy Efficient coverage control in WSNs based on ant colony Optimization" in International Symposium on Computer, Communication, Control and Automation 2010.

[8] S. Soro, and W. Heinzelman, "Prolonging LifeTime of Wireless Sensor Networks", Proceedings of the 19th IEEE International Parallel and Distributed Processing Symposium, IPDPS 05.

[9] J. Kennedy, R. Eberhart, "Particle swarm optimization," Proceedings of IEEE international conference on neural networks. Piscataway, NJ: IEEE ,pp. 1942-1948,1995.

[10] R. Eberhart, J. Kennedy, "A new optimizer using particle swarm theory," Proceedings Sixth Symposium on Micro Machine and Human Science.pp.39–43,1995.

[11] P. Brucker," On the complexity of clustering problems," Optimization and operations research, vol.157, pp., 1978. Micro sensor Networks", IEEE Transactions on Wireless Communications, vol. 1, pp. 660-670, 2002.

[12] M. Ye, C. F. Li, G. H. Chen, and J. Wu,"EECS: Energy Efficient Clustering Scheme in Wireless Sensor Networks", In Proceedings of IEEE Intl Performance Computing and Communications Conference, IPCCC 2005.

[13] F. Comeau, W. Robertson, S.C. Sivakumar and W.J. Phillips, "Energy Conserving Architectures and Algorithms for Wireless Sensor Networks", In Proceedings of 39th Hawaii International Conference on System Sciences, HICSS-39, 2006.

[14] Lunlei Bi, ZhiyuanLi, Ruchuan Wang," An Ant Colony Optimization-based Load Balancing Routing Algorithm for Wireless Multimedia Sensor Networks"

[15] Haosong Gou and Younghwan yoo, Hongqing Zeng, "A partition Based LEACH algorithm for wireless Sensor Networks", IEEE Ninth International Conference and Information Technology.2009.

[16] M.Dorigo,"Optimization, Learning and Natural Algorithms", PhD thesis, Italic, 1992.

The Use of Seismic Refraction Survey in Geotechnical Investigations

Bawuah, G.[1*]; Baffoe, E.[2*]; Darko, B.[3]; Hadir, I. A. A.[4]; Ogbetuo, D.[5]

Department of Geological Engineering, College of Engineering, Kwame Nkrumah University of Science and Technology, Ghana

*Corresponding authors

***Abstract*—** *The objective of this project was to use seismic refraction techniques to delineate the subsurface layers as a supplement to routine geotechnical investigations. Seismic velocities of the subsurface material were determined and used to find the possible composition of the subsurface materials and also to delineate the subsurface layers and their thicknesses. The seismic data was obtained using Geometric SmartSeis ST® 12-channel signal enhancement seismograph and Mark Product Limited® 48-Hz geophones. The survey was conducted along four traverse lines each with a length of 135m. It was determined from the seismic survey that the project site maybe underlain by dry loose sand, saturated sand and/or clay material. Information from two exploratory boreholes drilled to a maximum depth of 10.45m at the study area was consistent with the seismic refraction results obtained. The seismic results also showed there could be a fault at the project area along Traverse Line 1 and Traverse Line 2.*

***Keywords*— Boreholes, Geophones, Seismograph, Sesimic velocities, Subsurface.**

I. INTRODUCTION

Geophysics is the science concerned with the study of the physical processes and physical properties of the earth and its surrounding space environment. Although geophysics is mostly applied in geology, it may also be applied in several fields such as civil engineering, hydrology[1]. Geophysics has many disciplines with seismology being the largest, especially in exploration geophysics. Seismology may be either refraction or reflection seismology. Reflection seismology is currently the most commonly used geophysical method in oil and gas exploration even though seismic refraction was the first major geophysical method to be applied in the search of oil bearing structures. Seismic reflection offers a higher degree of technical sophistication in both data acquisition and signals processing even though it provides a 2 or 3 dimensional imagery of the stratigraphic boundaries and geological structures to depths of several kilometers into the earth. It can be used in shallow ground exploration but tend to be relatively expensive compared to electrical resistivity. Refraction seismology measures the arrival times of seismic waves at some fixed positions on the ground after its generation at the focus. For shallow seismic refraction investigations, a small explosive charge or sledge hammer can be used to generate the seismic energy, which moves through the subsurface at a velocity depending on the subsurface material. A part of the waves that travel through the subsurface are refracted at the interface between two layers back to the surface where it is detected by geophones at fixed locations. These signals are then sent to a seismograph which records the arrival times for the signals. The arrival time depends on the velocity of the waves in the layer it travels through and so with the time of arrival and the distance from the focus to the geophone known, the velocity of the wave can be determined. The velocity of a particular earth material can vary over a wide range as a function of its age, its depth of burial, its degree of fracturing or porosity, and whether water or air fills the voids[2]. The velocity variation can also aid in determining the number of layers the wave has travelled through and their elastic properties, thus informing the engineer or geologist on the kind of material to expect at different depths within the subsurface. This research seeks to use the Seismic Refraction Survey method to obtain the subsurface profile for the purpose of geotechnical investigations. Subsurface geotechnical investigations have been used in many cases to determine the properties of the subsurface materials at a site. The results from these investigations inform the engineer on the type and depth of foundation and even the type of excavating equipment to use at the site. Boreholes, trenches and other invasive methods are conventionally used to investigate the subsurface but these are discrete and may cause serious omissions in an attempt to delineate the boundaries of geological structures and the nature of the subsurface. This is a major issue in geotechnical investigation that seismic refraction survey addresses by giving a more continuous information of the subsurface based on which engineering decisions can be made with some degree of certainty. Seismic refraction survey also gives the various layers in the subsurface by using the velocities of the seismic waves in the subsurface thereby helping in reducing the number of borehole that are required for the subsurface investigation at a site. This reduces the cost involved in subsurface investigation. Like all geophysical methods, seismic refraction is non-diagnostic and a specific conclusion of the

material making up the subsurface cannot be drawn from the results of the seismic refraction survey alone. It is therefore very important that investigation is supplemented with some boreholes and knowledge of the geology of the area so that the possible material makeup of the subsurface can readily be inferred.

II. GEOLOGY AND PHYSIOGRAPHY OF STUDY AREA

The Kumasi metropolis is underlain predominantly by the middle Precambrian rocks specifically Birimian which comprises of the metasediments and metavolcanics. Also underlying the Kumasi metropolis are the granitoids that intruded and deformed the Birimian rocks [3]. The Kwame Nkrumah University of Science and Technology campus is underlain predominantly by the basin type granitoids. Figure 1 shows the geological setting of the study area. The Kumasi Metropolis falls within the sub-equatorial type with a minimum average temperature of about 21.5◦ and a maximum average temperature of 30.7◦. The average humidity in this area is about 84.16% at 0900GMT and 60% at 1500GMT. The Kumasi city falls within the moist semi-deciduous South-East Ecological zone with tree species such as ceida, triplochlon, celtis and other exotic species. The rich soil promotes agricultural activities generally [4].

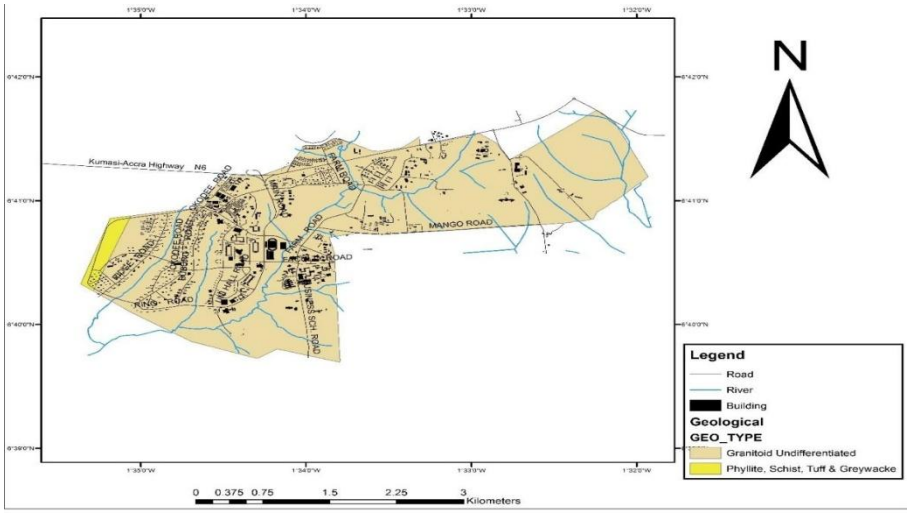

FIGURE 1. Geological Map of Knust

III. FIELD WORK AND DATA PROCESSING

The project was undertaken on the Kwame Nkrumah University of Science and Technology campus at a site in front of the now College of Arts premises. The project site was cleared for development but recently the surface is covered by fresh vegetation and the top soil is sandy material. The site was selected because of ease accessibility and the availability of some geotechnical data from boreholes drilled at the site, which was used to supplement the geophysical information. In order to determine the detailed subsurface profile, two traverse lines (Traverse Line 3 and Traverse Line 4) were chosen along slope and another two traverse lines (Traverse Line 1 and Traverse Line 2) across slope. **Figure 2** shows a plan view of the site with the traverse lines.

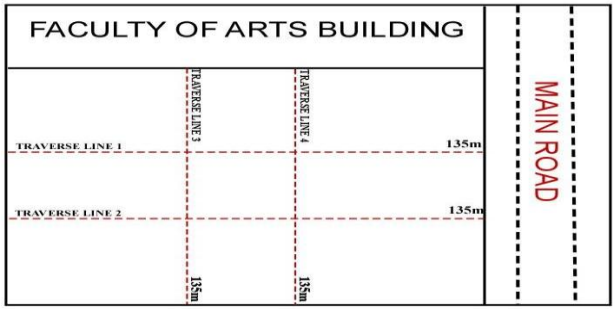

FIGURE 2. Plan View of the Study Area

3.1 Materials and Method Used

The main equipment used was the Geometrics SmartSeis ST-12-channel signal enhancement seismograph and its accessories including Mark Product Limited® 48-Hz geophones and the seismic cables. Also used were a hammer and a metallic plate to

generate seismic waves. The SmartSeis ST seismograph has the ability to filter disturbances of different amplitudes which are generated from other activities during the seismic field work other than the main waves generated by the impact. This filtering feature helps in producing clearer seismograms from which the first arrivals can be picked. The seismograph also has the ability to store seismograms allowing access after field work. The SmartSeis ST Seismograph can add up signals in a process called stacking which increase the amplitude of the waves that are generated. Stacking helps improve the signal-to-noise ratio as the ground is struck with hammer repeatedly. This generates clear seismograms from which the first arrivals can be picked. The hammer and metallic plate was used to generate the seismic waves because our investigations were shallow and all the other sources of seismic wave generation are expensive and others (explosives) in addition to been expensive, are very difficult to handle. The 12 geophones used gave a spread of 60m for the survey. The maximum depth of investigation in a seismic survey is estimated to be about one third of the geophone spread; the depth of our investigation is therefore about 20m which exceeds the usual depth of geotechnical investigation (10m). The seismic refraction survey was carried out by first marking the traverse line. The tape measure was spread along each traverse line and the shot points and geophone positions were marked off. For this research, the survey was done along four traverse lines. Two of these traverse lines were along slope and the other two were across the slope. Each traverse line was 135m in length and 6 shots were initiated along each traverse line. A forward shot (0m) and a reverse shot at (65m) and intermediate shots at (20m, 25m, 40m, and 45m). This was to give a better resolution of the subsurface along each traverse line. At the shot point, the sledge hammer was hit on a metal plate to generate the seismic waves. Staking was done twice so as to increase the intensity of the waves. This was repeated for all the shot points on all the traverse lines. The seismograph was used to record and store the seismogram from which the first break was picked. The filter system of the seismograph was used to eliminate noise of different intensities which was generated during the seismic survey.

IV. RESULTS AND DISCUSSION

The seismic survey investigation was conducted along four traverse lines as indicated in the methodology. The first arrival times were obtained from the seismograms that were generated by the SmartSeis ST Seismograph and plotted against the offset distances. The graphs displayed points that fall along distinct lines, the number of distinct lines shows the number of layers detected in the subsurface. The gradients of these lines were used to compute their velocities and thicknesses. **Figure 3** is a typical time-distance graph showing three layers with the equations of the distinct lines.

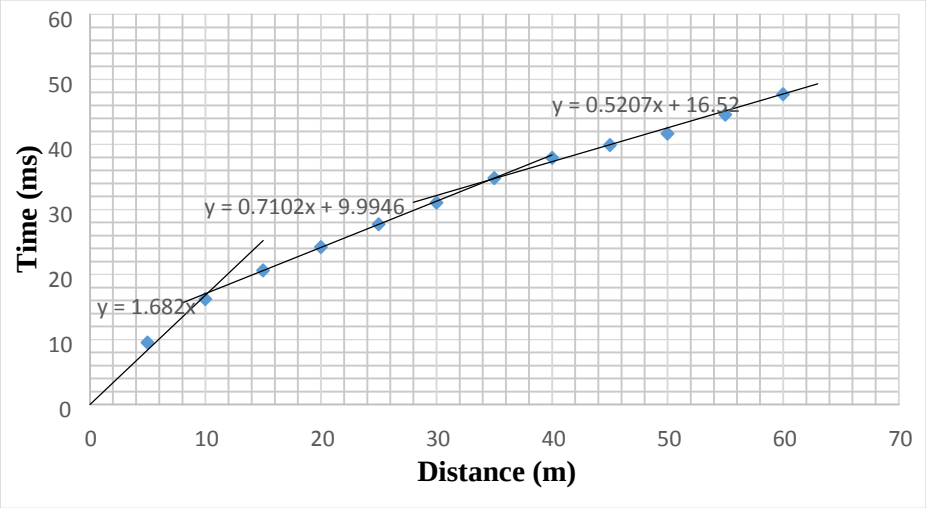

FIGURE 3. Distance Time Graph Obtained For Shot Point 40m along Traverse Line 4

From the graph in **Figure 3**, the velocity of each layer is given by the inverse of the gradient of the line representing that layer. The computations are as shown below:

$$V_1 = \frac{1000}{1.682} m/s = 594.5\, m/s$$

$$V_2 = \frac{1000}{0.710} m/s = 1408.5\ m/s$$

$$V_3 = \frac{10000}{0.521}\ m/s = 1912.2 \text{ m/s}$$

$$h_1 = \frac{t_1}{2} \times \frac{v_1 \times v_2}{\sqrt{v_2^2 - v_1^2}} h_2 = \frac{v_2 v_3}{\sqrt{v_3^2 - v_3^2}} \times \left(\frac{t_2}{2} - \frac{h_1 \sqrt{v_3^2 - v_1^2}}{v_1 \times v_3} \right)$$

$$h_1 = \frac{9.9994 \times 10^{-3}}{2} \times \frac{594.5 \times 1408.5}{\sqrt{1408.5^2 - 594.5^2}} = 3.3m$$

$$h_2 = \frac{1408.5 \times 1919.23}{\sqrt{1919.23^2 - 1408.5^2}} \times \left(\frac{16.52 \times 10^{-3}}{2} - \frac{3.3\sqrt{1919.23^2 - 594.5^2}}{594.5 \times 1919.23} \right) = 6.2m$$

TABLE 1
LAYERS DETECTED AT SHOT 40 M ALONG TRAVERSE LINE 4

SP	traverse	Layer	gradient	t_i(ms)	Velocity(m/s)	Thickness(m)
SP 40	Forward	1	1.682	0	594.5	3.3
		2	0.7102	9.995	1408.5	6.2
		3	0.5207	16.52	1919.23	

Based on the estimated velocities and thicknesses of the layers from the time-distance plots, the possible interpretations of the subsurface material and structures, of the study area are presented below.

4.1 Traverse Line 1

Table 6 shows the computation of velocities and thicknesses of the various layers along Traverse Line 1. The Traverse Line 1 reveals three layers with average velocities of 459.1, 1451.6, and 1718.3m/s for the first, second and third layers respectively. The velocities indicate that the first layer may be dry loose sand, the second layer saturated clay material and third layer may be made of saturated clay and sand material. **Figure 4** shows a simplified profile of the subsurface with the thicknesses of the various layers and the dip of the interface between the layers at areas along the Traverse Lines.

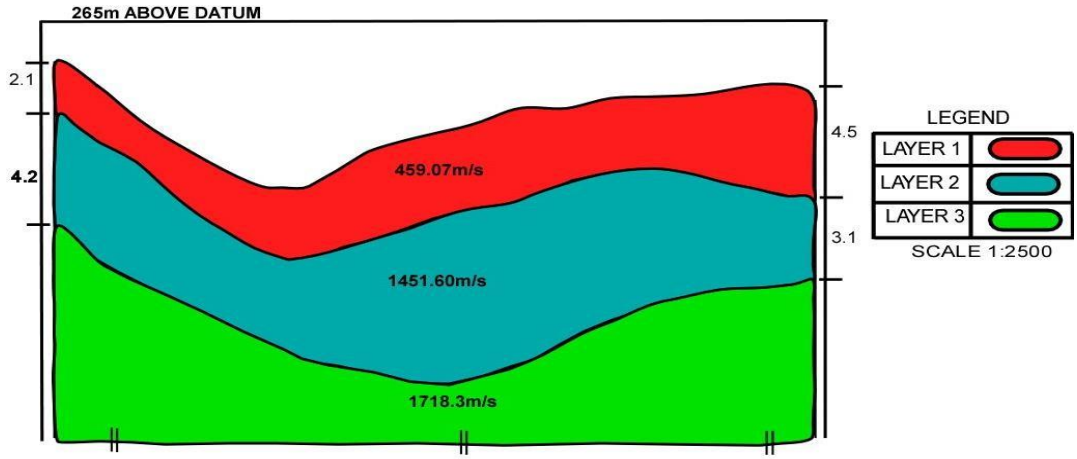

FIGURE 4: Subsurface Model Revealed by Traverse Line 1

4.2 Traverse Line 2

Three layers were realised in the subsurface along Traverse Line 2 with average velocities of 369.6, 1864.0, and 2103.0m/s for the first, second and third respectively as shown in the tabular representation of computations in **Table 7**. From the velocities obtained, the first layer is likely to be dry loose sand, whilst the second and third layers may be saturated clayey sand material with the second layer denser than the third layer. The graphs and the velocities obtained from the forward traverse indicate there may be a fault along this traverse line. **Figure 5** shows the nature of the subsurface with the thicknesses of the various layers and the dip of the interface between the layers at areas along the Traverse Lines.

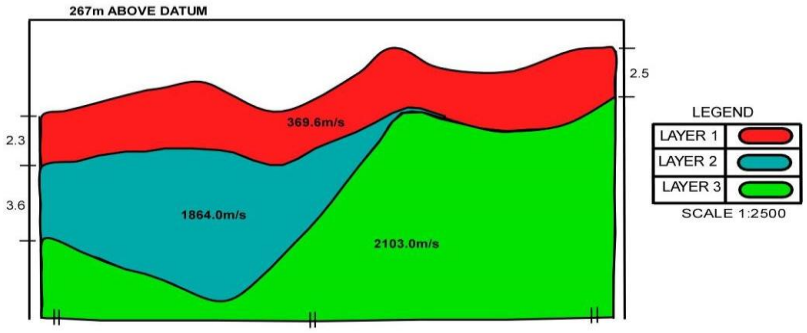

FIGURE 5. Subsurafce Model Revealed by Traverse Line 2

4.3 Traverse Line 3

Shown in **Table 8** is a tabular representation of the computation of velocities and thicknesses of the various layers along Traverse Line 3. Three layers with average velocities 794.6, 1427.2, and 1666.9m/s for layer 1, layer 2 and layer 3 respectively. These velocities indicate that the first layer may be compact sand material, the second layer saturated clay material and the third layer may be saturated clay and sand material. **Figure 6** shows the nature of the subsurface with the thicknesses of the various layers and the nature of the interface between the layers at areas along the Traverse Lines.

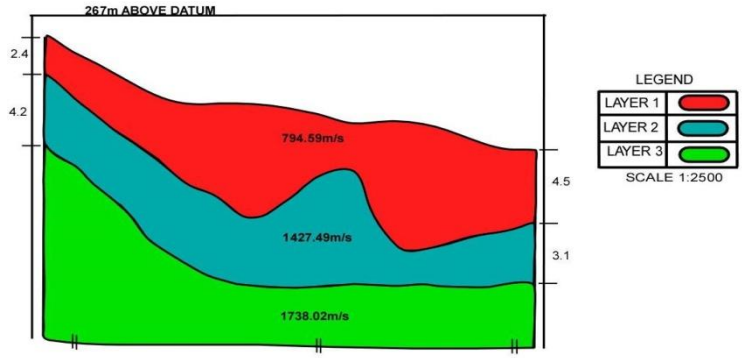

FIGURE 6. Subsurface Model Revealed by Traverse Line 3

4.4 Traverse Line 4

Shown in **Table 9** is a tabular representation of the computation of velocities and thicknesses of the various layers along traverse line 4. The traverse shows three layers with average velocities of 643.7, 1311.0, and 1344.7 m/s for the first, second and third layers respectively. From the velocities obtained, the first layer may be made of compact sand materials, the second and third layer may be saturated clay and sand material. **Figure 7** shows the nature of the subsurface with the thicknesses of the various layers and the dip of the interface between the layers at areas along the Traverse Lines.

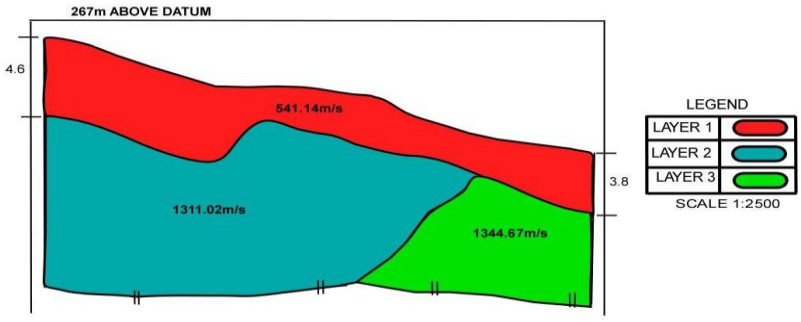

FIGURE 7. Subsurface Model Revealed By Traverse Line 4

V. CONCLUSION

From the analysis of the Time Distance graph, the project site may be underlain by three layers with average seismic velocities of the layers ranging from 369.6 to 2103.3m/s. The project site may therefore be underlain by dry loose sand,

saturated sand and clay material. Two exploratory boreholes with a maximum depth of 10.45m have been drilled at the site for investigation and the materials that were obtained from the boreholes are consistent with the materials detected in the subsurface by the seismic survey. Analysis of the graphs, **(Figure 11, Figure 14, and Figure 21)** indicates that there could be a fault at the project site specifically along Traverse Line 1 and Traverse Line 2. From the thicknesses obtained at the various shot points, models of the subsurface were generated as shown in **Figure 4, Figure 5, Figure 6 and Figure 7**. The thickness of the first layer was realized to fall between 2.1m to 7.2m. From the subsurface models, Traverse line 1 reveals three layers with the interfaces between the layers mimicking the topography as shown in the subsurface model in **Figure 4**. Traverse line 2 also reveals three layers with the interface between the first and second layer mimicking the topography along that traverse line. The break which is also detected from the Time Distance graphs **(Figure 14 and Figure 17)** also shows in the model of subsurface along this traverse line shown in **Figure 5**. Traverse Line 3 reveals three layers. The subsurface model as shown in **Figure 6** shows that there could be a fold of the second layer into the first layer making the interface between the first and second layer undulating. The thickness of the second layer reduces down slope (that is from shot point 0m because 65m) along this Traverse Line. The Time Distance graphs shown in **Figure 20, Figure 22, Figure 23**, and **Figure 24** indicate that, at some points along the distinct line representing the second layer, the refracted seismic waves have shorter or longer arrival times. This also shows that interface between the first and second layers could be undulating as shown in the subsurface as shown in the subsurface model in **Figure 6**. Three layers were realised in the subsurface along Traverse Line 4. The interface between the second and third layer is nearly vertical as shown in the subsurface model along this traverse line. The thickness of the first layer reduces down slope (that is from shot point 0m to shot point 65m). This is shown in the subsurface model shown in **Figure 7.**

TABLE 2
FIRST ARRIVAL TIMES MEASURED ALONG TRAVERSE LINE 1

X	SP 0m	SP 20m	SP 40m	X	SP 65m	SP 45m	SP 25m
5	14.05	12.73	11.76	60	47.06	47.76	48.64
10	19.5	18.26	18.7	55	44.42	44.86	46.18
15	23.79	21.33	21.77	50	41.26	41.96	43.54
20	27.74	24.84	25.99	45	39.07	39.33	40.65
25	32.22	28.44	29.76	40	36.87	37.05	38.36
30	35.29	31.96	32.22	35	34.15	33.98	35.99
35	38.19	35.12	34.85	30	31.34	30.64	33.1
40	41.96	37.93	38.63	25	28.44	27.3	30.64
45	45.04	40.65	40.38	20	25.11	24.23	27.3
50	47.32	43.28	45.48	15	22.04	20.89	23.79
55	50.57	46.62	49.51	10	18.7	17.38	20.02
60	54.61	50.57	55.92	5	10.89	11.33	12.03

TABLE 3
FIRST ARRIVAL TIMES MEASURED ALONG TRAVERSE LINE 2

X	SP 0m	SP 20m	SP 40m	X	SP 65m	SP 45m	SP 25m
5	13.61	14.66	13.25	60	40.38	41.26	41.7
10	18	20.02	19.58	55	38.63	39.51	39.77
15	20.02	23.09	22.47	50	36.43	37.49	37.49
20	21.6	26.25	26.25	45	32.66	34.15	35.12
25	23.97	28.88	29.32	40	30.9	31.52	32.66
30	26.86	31.52	32.66	35	28.88	29.06	29.76
35	29.5	34.15	35.73	30	27.13	26.86	28.01
40	31.96	36.87	38.36	25	24.84	23.97	25.28
45	33.98	38.89	39.95	20	22.21	21.6	23.35
50	35.99	40.65	42.58	15	20.02	19.31	20.19
55	38.19	42.4	45.74	10	17.82	16.68	17.82
60	41.26	45.04	48.81	5	13.5	12.2	14.22

TABLE 4
FIRST TIMES ARRIVAL MEASURED ALONG TRAVERSE 3

X	SP 0m	SP 20m	SP 40m	X	SP 65m	SP 45m	SP 25m
5	10.71	7.81	8.25	60	53.29	51.45	47.5
10	17.38	13.75	14.25	55	49.69	47.32	44.16
15	20.89	18.88	20	50	46.18	43.11	41.09
20	24.67	21.33	23.97	45	42.84	39.95	39.33
25	29.32	24.64	29.5	40	39.51	37.93	36.87
30	33.1	27.57	35.99	35	35.99	35.56	34.41
35	35.99	30.46	40	30	31.96	32.22	31.52
40	38.36	33.1	42.84	25	26.43	28.44	28.62
45	39.95	35.73	45.5	20	22.75	24.84	25.28
50	42.58	37.75	48.64	15	16.25	20.02	21.33
55	45.91	40.38	53.03	10	10.25	14.25	15.25
60	48.64	43.04	56.36	5	5.75	8.5	8.25

TABLE 5
FIRST TIME ARRIVAL MEASURED ALONG TRAVERSE LINE 5

X	SP 0m	SP 20m	SP 40m	X	SP 65m	SP 45m	SP 25m
5	13	10.71	9.57	60	61.89	54.78	53.03
10	19.5	18	16.24	55	56.36	50.83	48.64
15	26.86	24.41	20.63	50	51.27	46.18	44.87
20	31.78	29.76	24.23	45	46.18	43.72	41.53
25	36.43	34.15	27.74	40	41.7	40.82	38.36
30	39.51	37.75	31.08	35	38.63	37.93	35.12
35	43.11	40.21	34.85	30	35.12	34.15	31.78
40	47.06	43.98	37.93	25	31.34	29.76	28.18
45	50.39	48.2	39.95	20	26.86	25.81	24.41
50	54.34	51.97	41.7	15	22.47	21.33	20.89
55	58.56	55.22	44.6	10	16.86	16.68	16.86
60	64.35	59	47.76	5	11.33	10.27	11.59

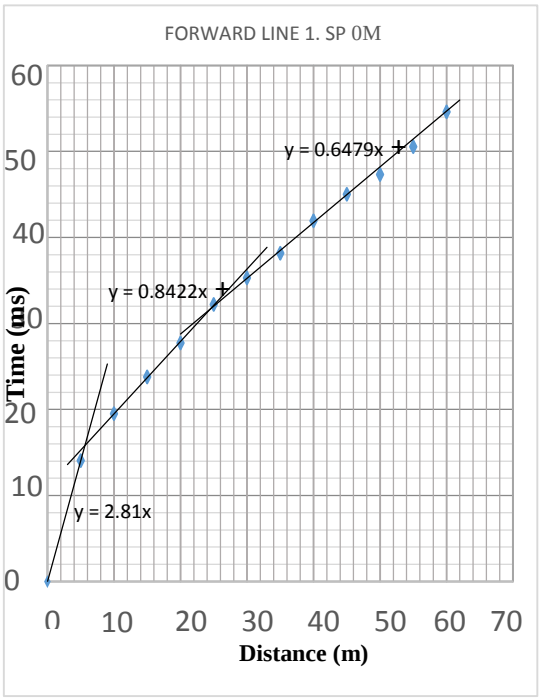

FIGURE 8

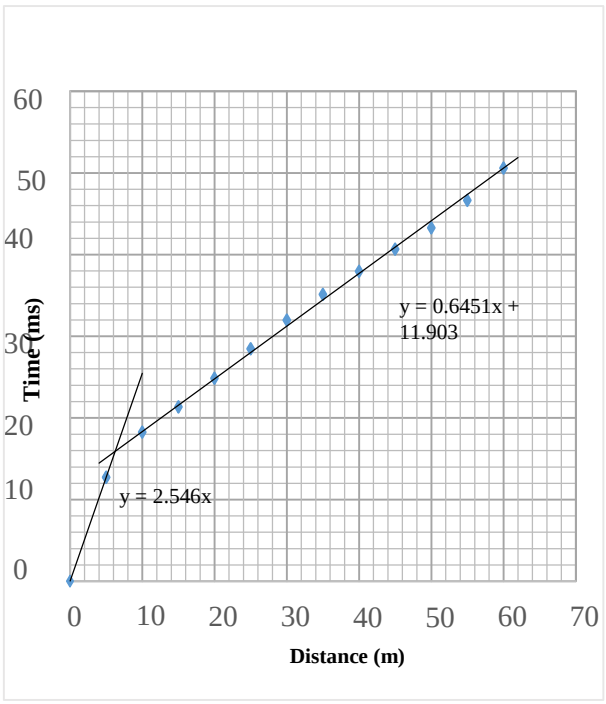

FIGURE 9

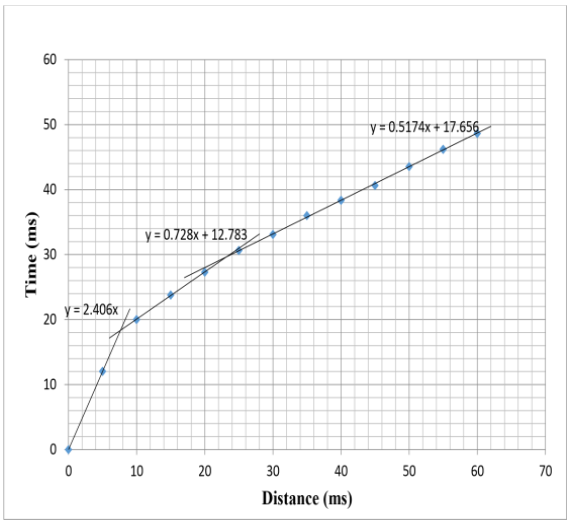

FIGURE 10

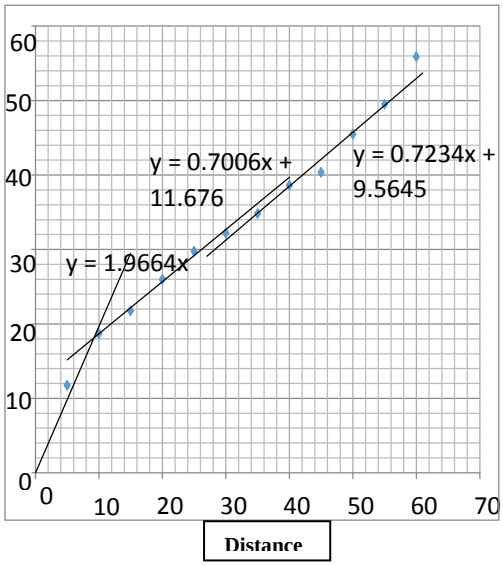

FIGURE 11

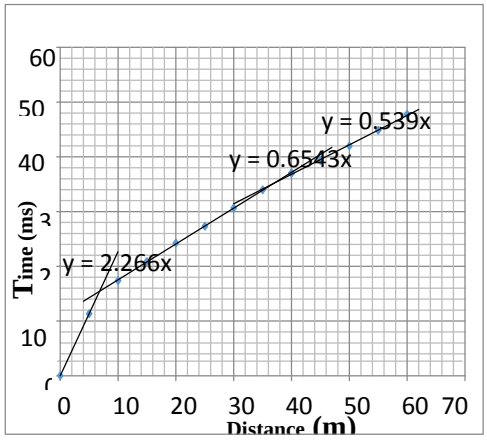

FIGURE 12

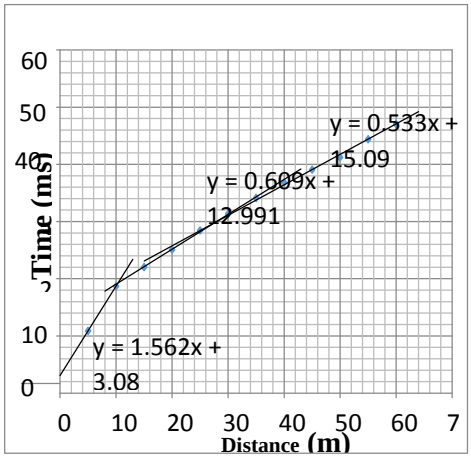

FIGURE 13

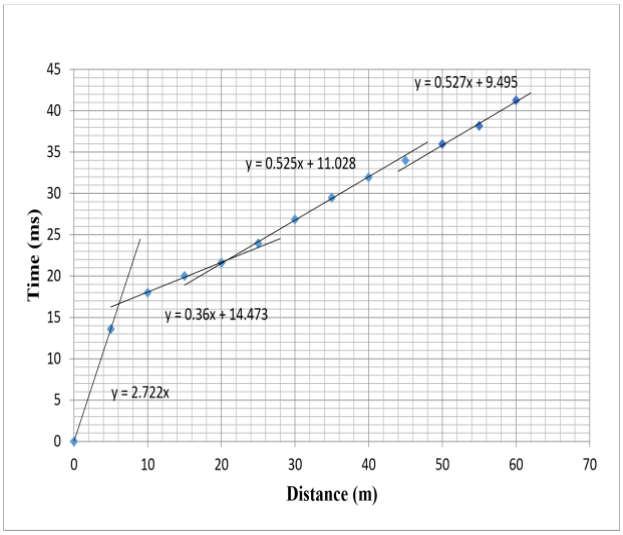

FIGURE 14

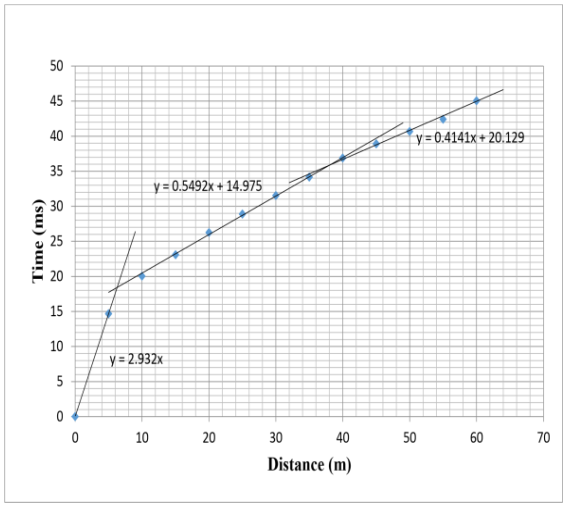

FIGURE 15

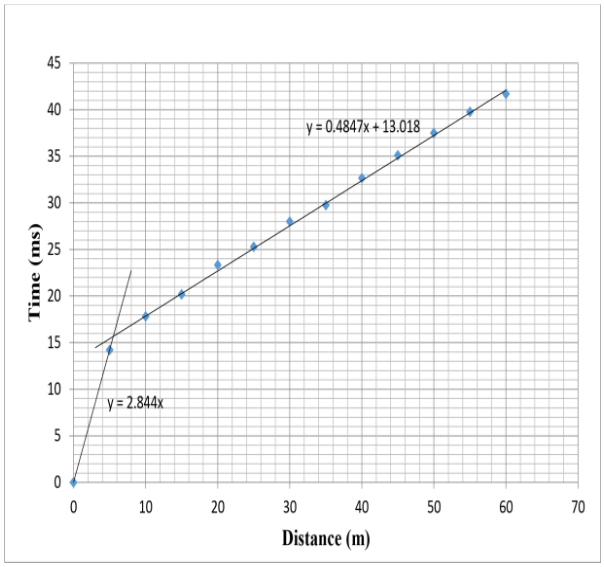

FIGURE 16

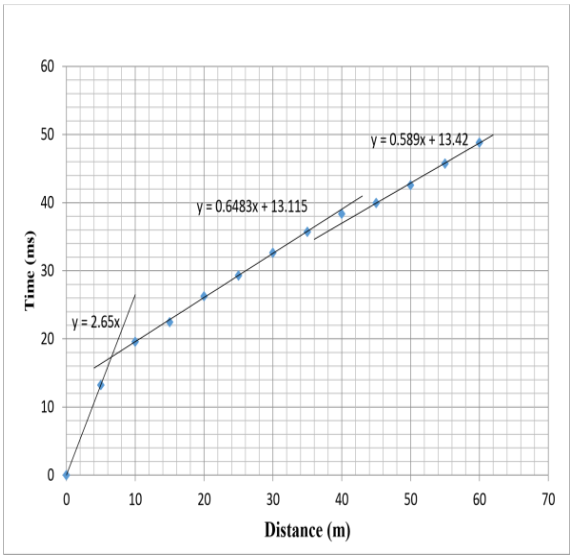

FIGURE 17

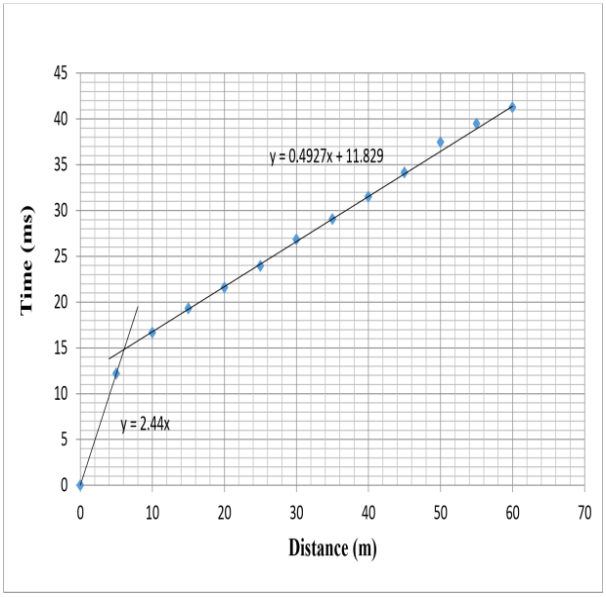

FIGURE 18

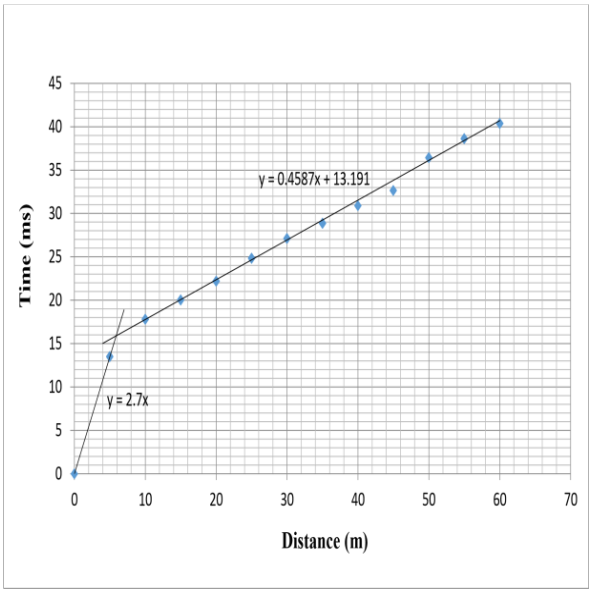

FIGURE 19

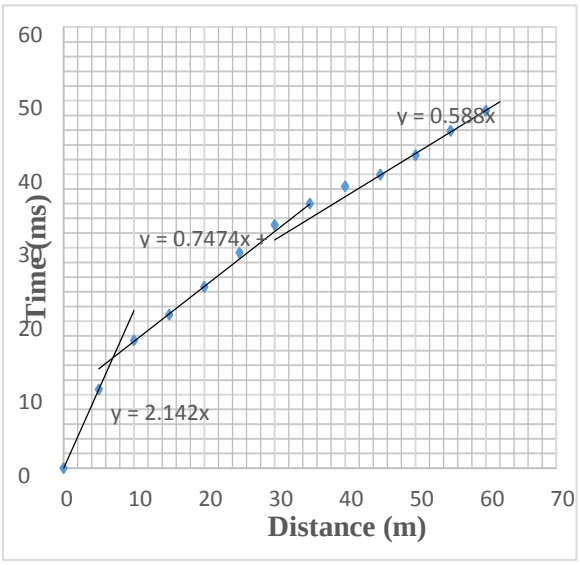

FIGURE 20

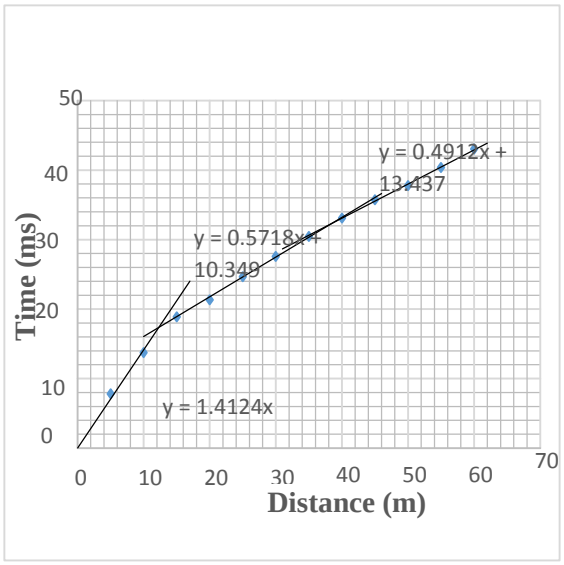

FIGURE 21

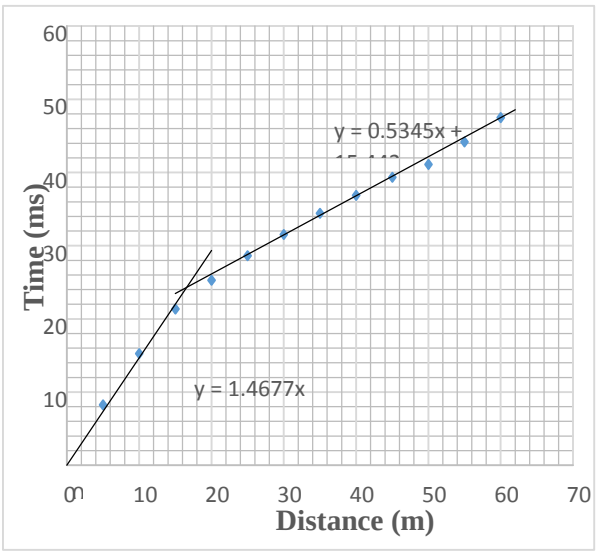

FIGURE 22

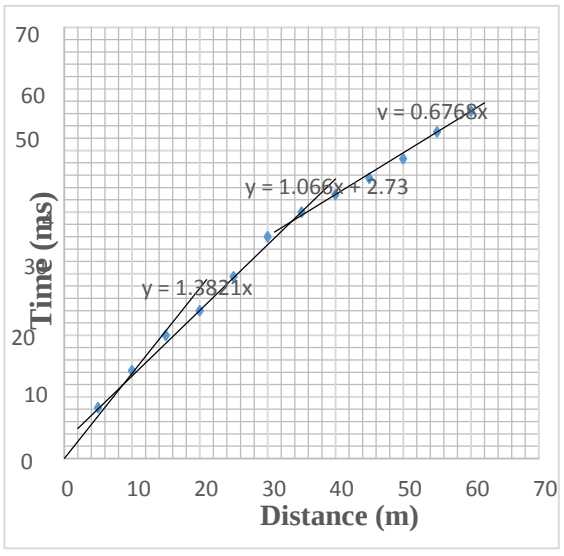

FIGURE 23

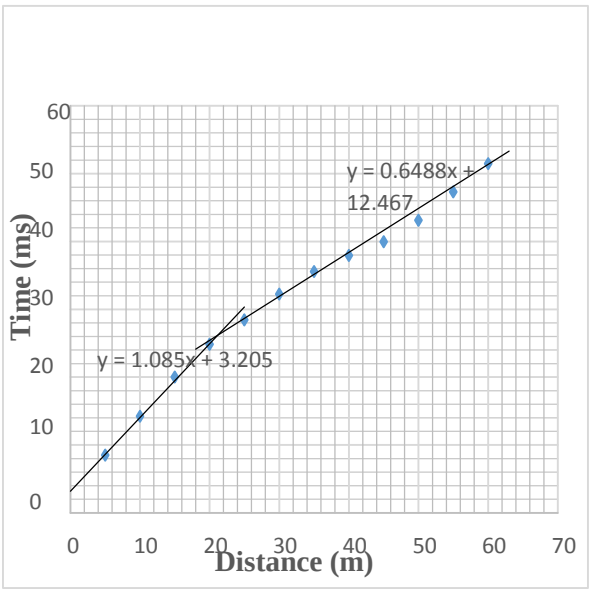

FIGURE 24

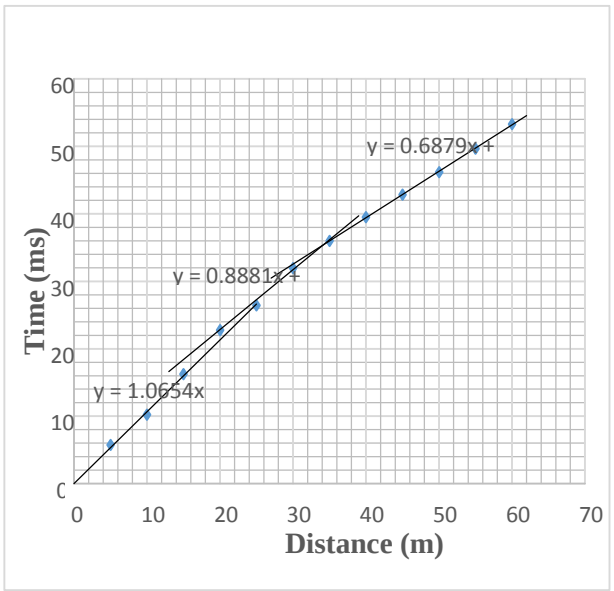

FIGURE 25

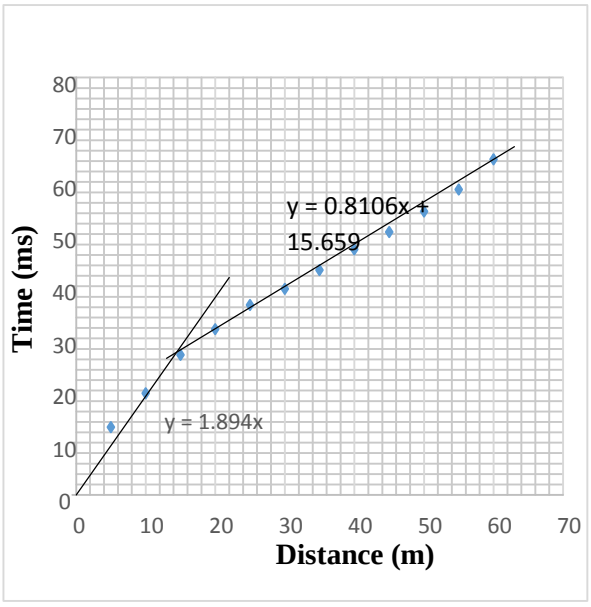

FIGURE 26

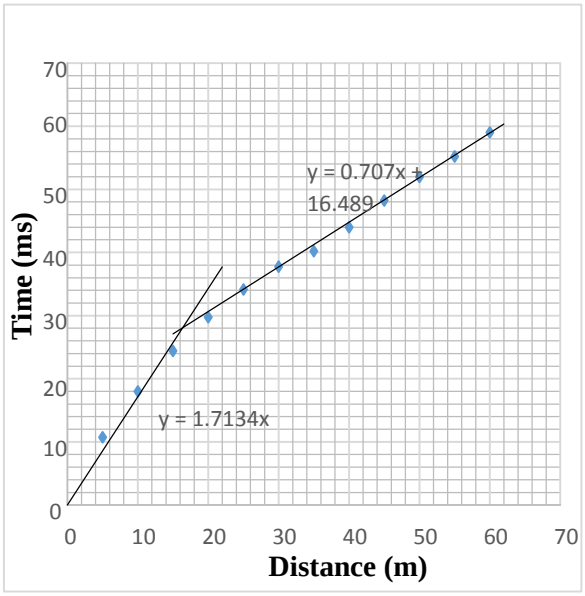

FIGURE 27

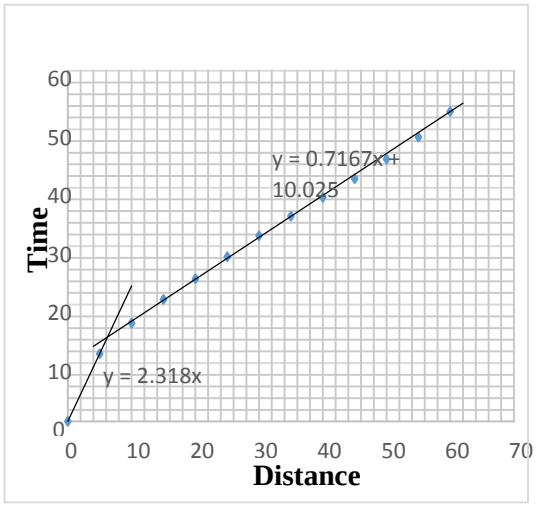

FIGURE 28

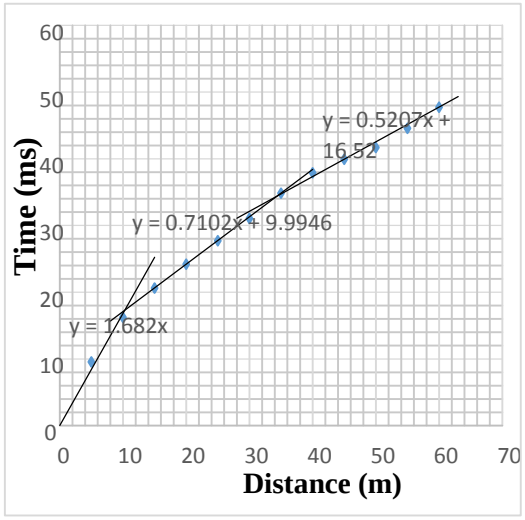

FIGURE 29

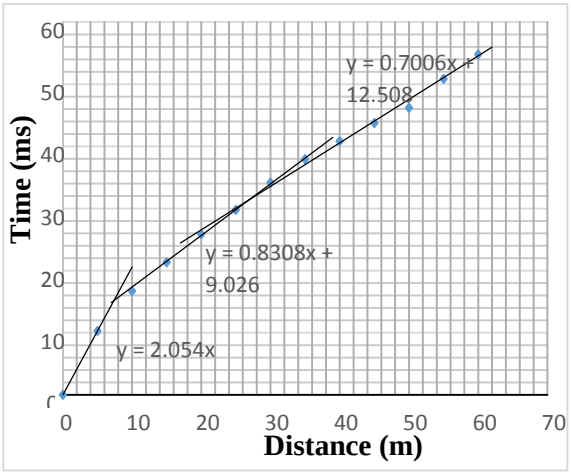

FIGURE 30

FIGURES 8-30: Show Distance Time Graphs Obtained For Shot Points 0 To 65m Each For The Traverse Lines

TABLE 6
SEISMIC COMPUTATIONS FOR TRAVERSE LINE 1

SP(m)	Traverse	Layer	Gradient	ti(ms)	V (m/s)	Thickness(m)	V_{avg}(m/s)
0	Forward	1	2.81	0	355.87	2.1	459.07
		2	0.8422	11.074	1187.37	4.2	1451.60
		3	0.6479	15.808	1543.45		1718.30
20	Forward	1	2.546	0	392.77	2.4	
		2	0.6451	11.903	1550.15		
25	Reverse	1	2.406	0	415.63	2.8	
		2	0.728	12.780	1373.63	4.4	
		3	0.517	17.650	1934.24		
40	Forward	1	1.966	0	508.65	3.2	
		2	0.7006	11.676	1427.35		
		3	0.7234		1382.36		
45	Reverse	1	2.266	0	441.31	2.5	
		2	0.654	10.990	1529.05	5.5	
		3	0.539	15.240	1855.29		
65	Reverse	1	1.562	0	640.20	4.5	
		2	0.609	12.990	1642.04	3.1	
		3	0.533	15.090	1876.17		

TABLE 7
SEISMIC COMPUTATIONS FOR TRAVERSE LINE 2

SP(m)	Traverse	Layer	Gradient	ti(ms)	V (m/s)	Thickness(m)	V_{avg}(m/s)
0	Forward	1	2.722	0	367.38	2.3	369.60
		2	0.493	12.09	2027.99	3.6	1863.96
		3	0.456	13.47	2192.02		2103.00
20	Forward	1	2.932	0	341.06	2.6	
		2	0.549	14.97	1821.49	7.0	
		3	0.414	20.12	2415.46		
25	Reverse	1	2.844	0	351.62	2.3	
		2	0.485	13.018	2063.13		
40	Forward	1	2.650	0	377.36	2.6	
		2	0.648	13.11	1543.21	0.4	
		3	0.589	13.42	1697.79		
45	Reverse	1	2.440	0	409.84	2.5	
		2	0.493	11.829	2029.63		
65	Reverse	1	2.700	0	370.37	2.5	
		2	0.459	13.191	2180.07		

TABLE 8
SEISMIC COMPUTATION FOR TRAVERSE LINE 3

SP(m)	Traverse	Layer	Gradient	ti(ms)	V (m/s)	Thickness(m)	V_{avg}(m/s)
0	Forward	1	2.142	0	466.85	2.4	794.59
		2	0.747	9.784	1337.97	3.6	1427.19
		3	0.588	13.4	1700.68		1666.94
20	Forward	1	1.188	0	841.75	5.0	
		2	0.572	10.349	1748.86	4.6	
		3	0.491	13.437	2035.83		
25	Reverse	1	1.308	0	764.53	6.5	
		2	0.535	15.442	1870.91		
40	Forward	1	1.175	0	851.06	2.8	
		2	1.066	2.73	938.09	6.4	
		3	0.677	15.777	1477.54		
45	Reverse	1	1.085	0	921.66	7.2	
		2	0.649	12.467	1541.31		
65	Reverse	1	1.085	0	921.66	4.1	
		2	0.888	5.0693	1126.00	4.5	
		3	0.688	11.909	1453.70		

TABLE 9
SEISMIC COMPUTATION FOR TRAVERSE LINE 4

SP(m)	Traverse	Layer	Gradient	ti(ms)	V (m/s)	Thickness(m)	V_{avg}(m/s)
0	Forward	1	1.894	0	527.98	4.6	541.14
		2	0.8106	15.659	1233.65		1311.02
		3	0.9307		1074.46		1344.67
20	Forward	1	1.713	0	583.77	5.3	
		2	0.707	16.489	1414.43		
25	Reverse	1	2.318	0	431.41	2.3	
		2	0.7167	10.025	1395.28		
40	Forward	1	1.682		594.53	3.3	
		2	0.71	9.995	1408.45	6.3	
		3	0.521	16.52	1919.39		
45	Reverse	1	2.054	0	486.85	2.4	
		2	0.8308	9.026	1203.66	3.6	
		3	0.7006	12.507	1427.35		
65	Reverse	1	1.607	0	622.28	3.8	
		2	0.826	10.457	1210.65		
		3	1.0444	0.9725	957.49		

VI. RECOMMENDATION

The occurrence of the fault in the study area, specifically along Traverse Line 1 and Traverse Line 2, should be investigated and considered in foundation design since it can result in differential settlement of structures. From our investigation, bedrock may not be encountered at the depth of investigation (approximately 20m). Excavations (commonly not more than 10m) at the site for geotechnical purposes can be done with the appropriate excavators like Tracked or Wheeled excavator or even a Backhoe.

REFERENCES

[1] Sheriff R. E.,Encyclopedic Dictionary of Applied Geophysics (Geophysical References No. 13), 3rd Edition, Society of Exploration Geophysics, ISBN 978-1-56080-018-7.

[2] Telford, W. M., Geldart, L. P., Sheriff, R. E., and Keys, D. A., Applied Geophysics, New York: Cambridge Press, 1976, pp. 860.

[3] Kesse, G. O., The Rock and Mineral Resources of Ghana, A. A. Balkema Rotterdam, The Netherlands, 1985, pp. 610.

[4] KMA, Climate and Vegetation, http://www.kma.ghanadistricts.gov.gh/climate,vegetation,geology.htm. (Accessed, November 23, 2015).

Copolymerization of (p-2-Ethoxycarbonyl) cyclopropyl Styrene with Glycidyl Methacrylate

K.G.Guliyev[1], A.I.Sadygova[2], S.B.Mamedli[3], Ts.D.Gulverdashvili[4], A.M.Aliyeva[5], D.B.Tagiyev[6]

[1,3,5]Institute of Polymer Materials of Azerbaijan National Academy of Sciences, Azerbaijan
[2,4,6]Azerbaijan Medical University, biophysical and bioorganic chemistry (sub) department, Azerbaijan

Abstract— *The radical copolymerization of (p-2-ethoxycarbonyl)cyclopropyl styrene with glycidyl methacrylate has been investigated. The new cyclopropane- and epoxy-containing photosensitive copolymers have been prepared. The constant values of relative activity of the monomers have been determined and the parameters Q-e on Alfrey and Price have been calculated. The copolymerization constants of this compound (r_1) with glycidyl methacrylate (r_2) calculated on Feynman-Ross method are: $r_1 = 1.15$, $r_2 = 0.42$, respectively; values of parameters Q and e: $Q_1 = 1.85$, $e_1 = -0.75$, respectively. The composition and structure have been established and the photochemical investigations of the synthesized copolymer have been carried out. It has been established that structuring proceeds due to opening of cyclopropane ring, epoxide and carbonyl groups.*

Keywords— copolymerization, (p-2-ethoxycarbonyl)cyclopropyl styrene, microstructure, monomers, photosensitivity.

I. INTRODUCTION

The rapidly increasing information volume requires the improvement of existence and the creation of new types of its recording, storage and reproduction. The search of non-silver materials for resists is considerably stimulated with exhaustion of the world's silver reserves, which as a result of one cycle of the photographic process is irretrievably lost by half.

The polymers and copolymers containing various reactive and photosensitive groups in the side chains possess valuable complex of properties and possibility of cross-linking under action of radiation, which allows preparing the resists on their basis used in microelectronics [1].

Due to this, a problem of the preparation of new types of photosensitive polymers for microelectronics causes a great interest of researchers [2-7]. Previously the solution of this problem was realized by us by polymerization of functionally substituted cyclopropyl styrenes [8-11].

The interest to preparation of such polymers has been stipulated due to the fact that in the formed macromolecules there are reactive functional groups of various nature in the form of suspensions in the side macrochain. As a result of copolymerization of the functional cyclopropane-containing vinyl compounds being one of the perspective reactive monomers, there have been synthesized the polymers containing cyclopropane groups regularly located in the side appendages to macrochain [12, 13].

This work has been devoted to the investigation of regularities of the copolymerization of (p-2-ethoxycarbonyl)cyclopropyl styrene (ECCPC) with glycidylmethacrylate (GMA) and study of properties of the copolymers prepared on their basis with the aim of creation of new negative photosentitive copolymers. A choice of these monomers has been stipulated by the fact that the concentration of double bonds and their chemical nature and also an availability of cyclopropane ring in combination with carbonyl and epoxide group in monomers in a decisive extent influence on such important photolithographic parameters of the resist as photosensitivity, adhesion, transparency, resolving ability about which a large experimental material accumulated to present time evidences.

ECCPC is the new reactive monomer, the formula and data of the synthesis and homopolymerization of which have been presented in work [11]. For copolymerization of the studied systems it is important to choose the conditions in which the polymerization would be proceeded only on vinyl group, and the reactive fragments would be remained unchanged in the side chain.

II. EXPERIMENTAL

The synthesis of ECCPC was carried out on methodology described in work [11].

The copolymerization of the synthesized ECCPC with GMA was carried out at 70°C in ampoules in the benzene solution in the presence of 0.2% (from total mass of monomers) of dinitrilazoisobutyric acid (AIBN). Total concentration of the initial monomers was constant and was 2.0 mol/l.% and a ratio of the initial monomers changed in the concentrations, shown in Table 1. The forming copolymer was doubly reprecipitated from benzene solution to methanol or sulphur ether and dried in vacuum (15-20 mm merc.c) at 30°C to constant mass. On the expiry of specified time (10-20 min) by addition of reaction mixture to methanol excess there have been isolated the copolymers with different composition of comonomers. The conversion of the samples of copolymers, for which there have been calculated the copolymerization constants, was 10%. The copolymer, being a white powder is well soluble in aromatic and chlorinated hydrocarbons. Elemental analysis $C_{21}H_{26}O_5$. Calculated: C 70.39%, H 7.26. Found: C 70.20, H 7.10. The characteristic viscosity was determined in benzene in Ubbelode viscometer ([η] = 1.08 dl/g).

The composition of copolymer was estimated on content of epoxide groups by chemical method, based on ability of epoxide ring to add HCl quantitatively.

The IR-spectra of copolymers were registered on spectrometer UR-20, the NMR-spectra – on spectrometer BS-487B Tesla (80 MHz) in the solution of deuterated chloroform.

For determination of photosensitivity of the polymer there have been made some compositions for copolymer at various concentrations (4-13% solutions). Applying a photoresist layer on the substrate was carried out in dust-free medium.

All solutions of the resists were applied on glass substrate by means of centrifuge at 2500 rev/min. After applying of the workpiece the photoresist is sustained for no less 20 min for increasing the adhesion of photoresist to the substrate. Then the photoresist is cut off on contour of the workpiece to prevent any film delamination.

The thickness of the prepared films-resists was measured with microinterferometers „LINNIKA". The resist layer thickness after its drying for 10 min at room temperature and for 20 min at 30-35°C/10 mm mer.c was from 0.20-0.25 mcm.

The composition of copolymer was estimated on content of epoxide groups by chemical method, based on ability of epoxide ring to add HCl quantitatively.

The IR-spectra of copolymers were registered on spectrometer UR-20, the NMR-spectra – on spectrometer BS-487B Tesla (80 MHz) in the solution of deuterated chloroform.

For determination of photosensitivity of the polymer there have been made some compositions for copolymer at various concentrations (4-13% solutions). Applying a photoresist layer on the substrate was carried out in dust-free medium.

All solutions of the resists were applied on glass substrate by means of centrifuge at 2500 rev/min. After applying of the workpiece the photoresist is sustained for no less 20 min for increasing the adhesion of photoresist to the substrate. Then the photoresist is cut off on contour of the workpiece to prevent any film delamination.

The thickness of the prepared films-resists was measured with microinterferometers „LINNIKA". The resist layer thickness after its drying for 10 min at room temperature and for 20 min at 30-35°C/10 mm mer.c was from 0.20-0.25 mcm.

The exposure of the workpieces with applied photoresist was realized on installation with point source of light through a photomask. The mercury lamp DPT-220 (current intensity 2.2A, distance from radiation source – 15 cm, mobile shutter rate of exponometer – 720 mm/h, exposure time 5-20 s) was used as a source of UV-irradiation.

TABLE 1

PARAMETERS OF COPOLYMERIZATION OF ECCPC (M_1) WITH GMA (M_2)

Composition of the initial mixture, mol.%		Epoxide number	Composition of copolymers, mol.%		r_1	r_2	Q_1	e_1	$r_1 \cdot r_2$	Microstructure of the copolymer		
ECCPC M_1	GMA M_2		ECCPC m_1	GMA m_2						L_{M_1}	L_{M_2}	R
90	10	0.98	91.53	8.47	1.15 ±0.03	0.42 ±0.02	1.85 ±0.01	-0.75 ±0.02	*0.483*	11.35	1.04	16.14
70	30	2.91	75.73	24.27						3.68	1.18	41.15
50	50	4.78	60.16	39.84						2.15	1.42	56.02
30	70	6.85	42.96	57.04						1.49	1.98	57.63
10	90	9.71	19.09	80.91						1.12	4.78	33.89

L_{M_1} and L_{M_2} – average length of blocks of monomers units; R – coefficient of Harwood blocking

The development was carried out in the jet installation. As the developer it was used the mixture dioxane:isopropyl alcohol – 1:2 at temperature 18-25°C.

A criterion of photosensitivity of the negative photoresists under UV-irradiation is the completeness of passage of the photochemical polymerization reactions (cross-linking) of molecules of base of the photoresist.

After exposure and development, the content of insoluble polymer was calculated on mass of the residue as a fact of formation of the cross-linked product.

Photosensitivity – value, inverse to the dose of UV-light absorbed by the photoresist, in other words, the dose necessary for the photoresist transfer to an insoluble state. It is measured in $cm^2(Wt \cdot s)^{-1} = cm^2 J^{-1}$:

$$S = \frac{1}{H} = \frac{1}{E \cdot t}$$

H – exposition (or irradiation dose by UV-light), J·cm

E – intensity, $Wt\ (cm^2)^{-1}$

t – duration of irradiation, s

III. RESULTS AND DISCUSSION

With the aim of establishment of composition and structure of the synthesized copolymer the elemental and spectral (IR- and NMR-spectroscopy) analyses of the synthesized monomer and polymer samples have been carried out.

In view of the fact that ECCPC is the polyfucntional compounds, at its radical copolymerization with GMA it should be expected the formation of new reactive polyfunctional copolymer.

In the IR-spectra of the prepared copolymers on the basis of ECCPC with GMA there are observed the absorption bands, which can be used for structural characteristics of copolymers.

It has been established by comparison of IR-spectra of the copolymers with spectra of the initial monomer (ECCPC) that the absorption bands in the IR-spectrum of the initial monomer at 990 and 1640 cm^{-1}, referring to deformation and valence vibrations of double bond of the vinyl group after copolymerization disappear. The absorption bands characteristic for benzene ring (1410-1460; 1500-1600 cm^{-1}) and cyclopropane group (1030-1035 cm^{-1}) and also absorption bands at 1720, 1030 and 1110 cm^{-1}, referring to vibrations of carbonyl groups and ether bond, respectively, remain unaffected. In the spectrum of the copolymer there are also the characteristic frequencies of absorption belonging to epoxide ring (830-850,1250-1260 cm^{-1}) preserved after polymerization.

In the NMR-spectrum of copolymer the resonance signals referring to protons of benzene nuclei (δ = 6.60-7.30 ppm) and cyclopropane ring (δ = 0.65-1.66 ppm.) are clearly appeared, but the signals referring to protons of vinyl group (δ = 5.10-6.65 ppm.) – are absent. The protons of epoxide ring are characterized by signals at 2.30-2.60 ppm (–CH_2–) and at 2.96 ppm (–CH–). According to the data of spectroscopy, the copolymerization of ECCPC with GMA proceeds only due opening of double bonds of vinyl groups with preservation of other reactive functional fragments of both monomers. Thus, on the basis of analysis of IR- and NMR-spectra of the copolymers prepared by copolymerization of ECCPC with GMA, the following structure of copolymer is supposed:

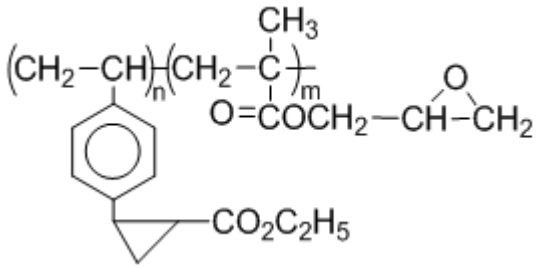

The copolymerization was carried out at various ratios of the initial monomers.

The initial composition is the main factor determining characteristics of the polymers. It has been revealed that the composition of forming copolymers depends on composition of the initial monomer mixture.

For estimation of the polymerization activity of ECCPC there have been calculated the constant values of relative activity of monomers on compositions of the initial monomer mixture on Feynman-Ross method [14] and parameters Q-e – on Alfrey and Price. The parameters of microstructure of the copolymers were determined based on copolymerization constant [15]. The obtained data are presented in Table 1.

The constant of values of relative activity (Table 1) evidence about the largest reactivity of ECCPC in comparison with GMA, which has been connected with influence of cyclopropane ring $–CO_2C_2H_5$ on electron density of double bond of the vinyl group [16]. The ester group is included in total system of conjugation causing redistribution of electron density both in monomer and in radical center forming from it. As a result a quantity of the energy necessary for occurrence of transition state is decreased leading to increase of the reactivity of monomer.

The calculated values of parameters of Q_1 and e_1 at copolymerization with GMA indicate to increased conjugation in monomer (ECCPC) connected with influence of substituent of $–CO_2C_2H_5$ fragment stipulating relatively high reactivity of monomer and more low reactivity of radicals. In calculation of factor e_1 it was chosen a negative sign, based on the fact that the electronic density of the double bond of the vinyl group of ECCPC should be less than in GMA, since an influence of substituent of ECCPC leads to the redistribution of density of electron cloud of double bond of the vinyl group changing the polarity of radical. It has been connected with this the large reactivity of ECCPC confirmed by copolymerization constant (r_1=1.15, r_2=0.42, respectively) in comparison with GMA. On the basis of calculated copolymerization constants the data about microstructure of copolymers have been obtained (Table 1). A length of blocks L_{M_1} is increased with increase of share of ECCPC in the composition of copolymer. It is seen from Table that R and L_{M_1} are maximum (56.02 and 57.63; 2.15 and 1.49 units, respectively) at ratio of the initial monomers 50:50, 30:70. It follows from here that by selection of the determined compositions of the monomer mixtures one can carry out the directed formation of microstructure of copolymers, which is one of the most perspective ways of modification of their properties.

An availability of the synthesized copolymer of reactive groups of various chemical nature in links of macromolecule causes an interest to investigation of the photochemical structuring of this copolymer, i.e. to cross-linking under action of UV-irradiation.

The photochemical investigations of the synthesized copolymers were carried out on methodology [9]. Owing to availability of groups strongly absorbing the light energy (cyclopropane, glycidyl, > C = O etc.) the synthesized copolymers are the photosensitive (55 cm^2J^{-1}) and under the influence of UV-irradiation are subjected to the photochemical conversions leading to the formation of net structures.

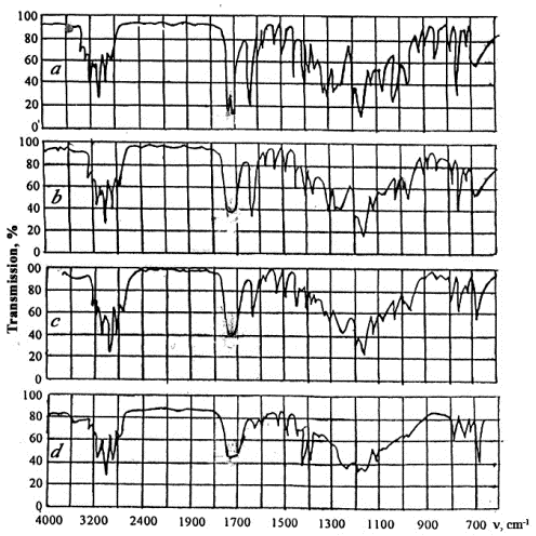

FIGURE 1: IR-SPECTRA OF THE COPOLYMER FILM OF ECCPC WITH GMA : UNIRRADIATED (A) AND IRRADIATED FOR 1-ST (B), 3-RD (C) AND 4-TH (D) MIN. M_1 : M_2 = 75.73 : 24.27 MOL%.

The structuring process of the prepared cyclopropane-containing copolymers has been studied by IR-spectroscopic investigations (fig.1). Depending on duration of irradiation, an intensity of maxima of the absorption bands characteristic for cyclopropane ring (1030-1035 cm^{-1}), carbonyl group (1720 cm^{-1}) and epoxide ring (830, 920, 1260 cm^{-1}) is changed; with

increase of irradiation time (more 3 min.) an intensity of maxima of the absorption bands of the indicated fragments are decreased and at irradiation ~ 5 min it practically disappear (fig. 2).

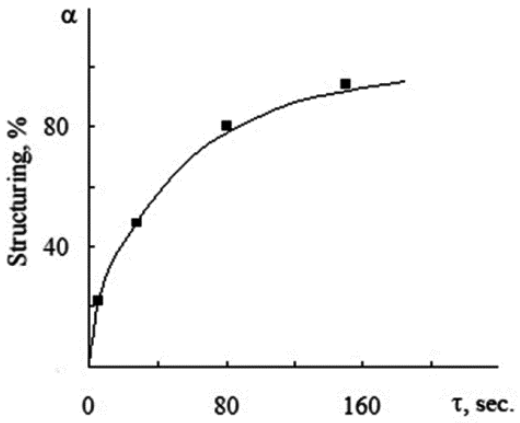

FIGURE 2: DEPENDENCE OF STRUCTURING ON IRRADIATION TIME OF THE COPOLYMER

Structuring proceeds due to opening of cyclopropane ring, carbonyl group and glycidyl fragments.

In the irradiation process on change of values of epoxide number the content of epoxide groups in the copolymer controlled [14].

Thus, an availability of cyclopropane ring, ethoxy carbonyl and glycidyl groups in macromolecules of the prepared copolymer allowed to create the material with high photosensitivity on the basis of copolymer.

As a result of carried out work the new copolymer has been synthesized and its composition, structure and properties have been established. It can be concluded on the basis of the carried out investigations that an availability of cyclopropane ring and glycidyl fragment in the structure of the new synthesized copolymer provides high photosensitivity, creation of a solid elastic layer with good adhesion to substrates and low microdefects of the polymer films for these copolymers.

IV. CONCLUSIONS

1. The radical copolymerization of (p-2-ethoxycarbonyl)cyclopropyl styrene with glycidyl methacrylate has been investigated. The new cyclopropane- and epoxy-containing photosensitive copolymers have been prepared.
2. The constant values of relative activity of the monomers have been determined and the parameters Q-e on Alfrey and Price have been calculated.
3. The composition and structure have been established and the photochemical investigations of the synthesized copolymer have been carried out.
4. It has been established that structuring proceeds due to opening of cyclopropane ring, epoxide and carbonyl groups.

REFERENCES

[1] Yu. S. Bokov, Photo-, electron- and X-ray resist. M.: Radio and communication, 1982.

[2] V. H. Filichkina, "Application of transparent plastic materials in the construction of capitalist countries," Chem. Industry abroad, pp. 11-27, November 1985.

[3] V. G. Rupyshev, M. P. Ivanko, G. I. Kozlova, E. I. Shepurev, N. B. Kariglazova, and V. M. Galperin, "Styrene copolymers with refractive index more 1.6," Plast.mass., pp. 58-59, March 1983.

[4] P. K. Tsarev, V. G. Baranov, and Yu. S. Lipatov, "Investigation of distribution of density on the surface layer of amorphous polymers," High-molecular compounds, vol. B12, pp. 115-117, February 1970.

[5] A. Ya. Vayner, and K. M. Dyumaev, "Negative photoresists on the basis of unsaturated derivatives of polyamidoacids," Chem. industry, p. 3, July 1989.

[6] A. Ya. Vainer, K. M. Dyumaev, I. A. Likhachev, A. D. Shalatonova, and Yu. A. Yartsev, "Methacrylate Derivatives of Carboxyl-Containing Polyimides: Synthesis and Photochemical Transformations," Doklady Physical Chemistry, vol. 396, pp. 115-118, January-March 2004.

[7] H. Hou, J. Jiang, and M. Ding, "Ester-type precursor of polyimide and photosensitivity," Eur. Polym. J., vol. 35, pp. 1993-2000,

November 1999.

[8] K. G. Guliyev, G. Z. Ponomareva, and A. M. Guliyev, "Photosensitivity of polymers on the basis of epoxy substituted vinylphenylcyclopropanes," Russian Journal of Applied Chemistry, vol. 79, pp. 488-491, March 2006.

[9] K. G. Guliyev, G. Z. Ponomareva, and A. M. Guliyev, "Synthesis and properties of epoxy-containing polycyclopropyl styrenes," Polymer Science, vol. B49, pp. 196-199, August 2007.

[10] K. G. Guliyev, S. B. Mamedli, and G. Z. Ponomareva, "Copolymerization of 2-alkoxymethyl-1(p-vinylphenyl)cyclopropanes with styrene," Processes of Petrochemistry and Oil-refining, vol. 10, pp. 183-186, February 2009.

[11] K. G. Guliyev, Kh. G. Nazaraliyev, and A. M. Guliyev, "Synthesis and polymerization of p-(2-functionally substituted)cyclopropyl styrenes," Azerb. Chem. J., pp. 87-90, January 1999.

[12] K. G. Guliyev, "Copolymerization of p-(2,2-Dichlorocyclopropyl)styrene with Methyl Methacrylate and Properties of the Resulting Copolymers," Russian Journal of Applied Chemistry, vol. 84, pp. 2114-2118, December 2011.

[13] K. G. Guliyev, G. Z. Ponomareva, and A. M. Guliyev, "Influence of substituents on copolymerization of p(2-substituted)cyclopropyl styrenes with methylmethacrylate," Processes of Petrochemistry and Oil-refining, pp. 40-43, January 2003.

[14] E. V. Kuznetsov, S. M. Divgun, , L. A. Budarina; N. I. Avvakumova, V. F. Kurenkov. Practical work on chemistry and physics on polymers. M.: Khimiya, 1977.

[15] E. N. Zilberman, "Parameters of microstructure of multi-component copolymers," High-molecular compounds, vol. B21, pp. 33-36, January 1979.

[16] K. G. Guliyev, G. Z. Ponomareva, S. B. Mamedli, and A. M. Guliyev, "Ultraviolet absorption spectra of 2-substituted-1(n-vinylphenyl)cyclopropanes," Journal of Structural Chemistry, vol. 50, pp. 693-695, August 2009.

Increase Kitchen Garden Productivity using IOT and Virtuino app

Prof (Dr). Jayant Shekhar[1], Mr. Desalegn Abebaw[2], Dr. Mesfin Abebe Haile[3]

[1]Prof(Dr).Jayant Shekhar,Professor, Adama Science and Technology University, Adama
[2]Mr. Desalegn Abebaw,CSE-Programe Chair, Adama Science and Technology University, Adama,
[3]Dr. Mesfin Abebe Haile ,CSE-PG-Coordinator, Adama Science and Technology University, Adama

Abstract— *Continuously increasing food prices of basic kitchen items, fruits and vegetables the poor and fixed income groups are suffering from the decreasing real incomes and purchasing power. The marginal increase in the income of the poor people to enable them to gain access to food and improve their nutrition is the need of the present time. The kitchen garden falls under bio-intensive and participatory innovation which can provide year round availability, access and consumption of adequate amount and varieties which supply not only the calorific demands but also the micronutrients by the resource poor. One of the easiest ways of ensuring access to a healthy diet that contains adequate macro- and micronutrients is to produce many different kinds of foods in the home garden. This is especially important in rural areas where people have limited income-earning opportunities and poor access to markets. Kitchen gardening contributes to household food security by providing direct access to food that can be harvested, prepared and fed to family members, often on a daily basis. Kitchen gardens can be grown in the empty space available at the backyard of the house or a group of women can come together, identify a common place or land and grow desired vegetables, fruits, cereals etc that can benefit the women and community as a whole. This leads to give the idea of automated kitchen gardening system. The system is designed to sense soil moisture and amount of light falling on the plants. When the moisture content in the soil is too low, the system will give command to start a pump and water the soil. Apart from this the Arduino and ESP8266 it will transmit information on moisture level and ambient light. You can monitor all the data from your smart phone by using Virtuino app. Then a twit can be send to your account automatically if the moisture falls below a given threshold value. It provides full control and monitoring of variables such as temperature, pest management and control works and more.*

Keywords— Vegetables, kitchen garden, urban areas, Arduino and ESP8266.

I. INTRODUCTION

In Euthopia and world over high population growth, rural urban migration and vulgarities of weather have pushed the cost of food upwards (Silvia, 2012). The increased use of food crops in biodiesel production put further imbalance to food supply which further affects the demand/supply relationship. Non-communicable diseases add further pressure to the citizens and more so to low income groups. The resultant of this is more people are going to be food insecure. Famine Early Warning system warned that there will be a rise from 2.2 million to 2.4 million food insecure people in August 2012 (UN, 2012).

The answer to increased food demand cannot be met by the green revolution as well as rain fed agriculture which is already showing fatigue (Pastakia, 2011) This food insecure group needs to face the *c*urrent environmental and health challenges by identifying ways to better align aesthetics, ecology, and health (Denver Urban Gardens, 2012). A kitchen garden can be a part of the solution to this problem. As already proven one-size-fits all solutions cannot be applied in every area to answer the question of food sustainability (Beddington, 2011).

The higher demand for food should be met by practical innovations like kitchen gardening which not only improves availability but also answers the question of diversity required for a healthy community. The kitchen gardens can be viewed as an adaptive strategy of communities as an entry point for development. The kitchen garden can also help to reduce the gap of productivity between the technical potential and actual production levels of food crops due to low use of suboptimal inputs and low adoption of most productive technologies (Tittonell, 2012). A kitchen garden involves the very people who are the greatest resource for development in a view to improve their own livelihoods and empowerment as envisaged in the rural university concept (Mathai, 1985). The kitchen gardening is a radical transformation towards using resources more efficiently. The kitchen garden is perhaps the only available ecological space available to the poor to meet their economic needs especially so in Africa where the poor tends to rely more on natural resource base for their livelihood. Kitchen Gardens depend on the gardeners for maintenance and are spaces made meaningful by the actions of people during the course of their every-day lives. They are spaces where the gains from social capital, physical and symbolic arrangement of items of private

living space are aggregated and given utility value. Above all, Kitchen garden is an avenue where the actor is totally immersed in his role (Kimber, 2012).

The British and the Americans won two world wars by growing their own food to feed their armies and the people left at home (Great Britain Ministry of Food, 1946). Euthopians can feed themselves by growing what we eat and one way to do this is adopting the Kitchen garden. The kitchen garden is a form of Community adaptive strategies that leads to sustainable livelihoods (Agobia, 1999).

A kitchen garden is an integrated system which comprises the family house, a recreational area and a garden producing a variety of foods including vegetables, fruits and medicinal plants for home consumption or sale. The kitchen gardens have been found to play an important role in improving food security for the resource poor rural households in developing country like Bangladesh (Asaduzzaman, 2011) and can do the same in Euthopia.

II. WHY IOT

Internet of Things (IoT) is a broad term that describes the interconnection of different daily life objects through the internet. In the concept of IoT every object is connected with each other through a unique identifier so that it can transfer data over the network without a human to the human interaction [1, 8]. IoT has referred as a network of everyday objects having ubiquitous computing. The ubiquity of the objects has increased by integrating every object with embedded system for interaction [9]. It connects human and devices through a highly distributed network. Due to enormous growth in technologies, farming has become more popular and significant. Different tools and techniques are available for development of farming. According to the UN Food and Agriculture Organization, in order to feed the growing population of the Earth, the world will need to produce 70% more food in 2050 than it did now. To meet this demand, farmers and agricultural companies are turning to the Internet of Things for analytics and greater production capabilities. Internet of Things (IoT) can play big role in increasing productivity, obtaining huge global market, idea about recent trends of crops. IoT is a network of interconnected devices which can transfer data efficiently without human involvement.

Today many agricultural industries turned to adopt IoT technology for smart farming to enhance efficiency, productivity, global market and other features such as minimum human intervention, time and cost etc. The advancement in the technology ensures that the sensors are getting smaller, sophisticated and more economic. The networks are also easily accessible globally so that smart farming can be achieved with full pledge. Focusing on encouraging innovation in agriculture, smart farming is the answer to the problems that this industry is currently facing. All this can be done using smart phones and IoT devices. Farmer can get any required data or information as well can monitor his agricultural sector.

In Internet of things, we can represent things with natural way just like normal human being, like sensor, like car driver etc. This thing is assigned an ip address so that it can transfer data over a network. As per the report generated by Garner, at the end of 2016 there will be 30% rise in count of connected devices as compared to 2015. He further says that, this count will increase to 26 billion by 2020[10]. The IoT technology is more efficient due to following reasons: 1. Global Connectivity through any devices. 2. Minimum human efforts 3. Faster Access 4. Time Efficiency 5. Efficient Communication.

The proposed system can be used for.

1. Garden water management
2. Pest management and control works

2.1 Garden water management

- Usually the we pumps the water more or less to cultivate the land.
- This may result in wastage of water or insufficiency to the garden.
- To prevent such situation INTERNET OF THINGS has a system that sends an alerting message to the owner when the moisture level increases or decreases.

2.2 Pest management and control works

- Often our hard work is destroyed by predators (pests) that results in huge loss to us.
- To prevent such situation INTERNET OF THINGS has a system that detects the motion of predators using PIR sensors.

- This information can be used by the owner to reduce damage done by predators.

III. IOT BASED GARDENING

Technological innovation in farming is nothing new. Handheld tools were the standards hundreds of years ago, and then the Industrial Revolution brought about the cotton gin. The 1800s brought about grain elevators, chemical fertilizers, and the first gas-powered tractor. Fast forward to the late 1900s, when farmers start using satellites to plan their work.

The IoT is set to push the future of farming to the next level. Here in the field section, various sensors are deployed in the field like temperature sensor, moisture sensor and PIR sensor. The data collected from these sensors are connected to the microcontroller through ESP8266.

In control section, the received data is verified with the threshold values. If the data exceeds the threshold value the buzzer is switched ON and the LED starts to blink. This alarm is sent as a message to the farmer and automatically the power is switched OFF after sensing. The values are generated in the thing speak web page and the farmer gets the detailed description of the values.

In manual mode, the user has to switch ON and OFF the microcontroller by pressing the button in the Android Application developed. This is done with the help of Virtuino app.

In automatic mode, the microcontroller gets switched ON and OFF automatically if the value exceeds the threshold point. Soon after the microcontroller is started, automatically an alert must be sent to the user. This is achieved by sending a message to the user through the Virtuino app.

Other parameters like the temperature, humidity, moisture and the PIR sensors shows the threshold value and the water level sensor is used just to indicate the level of water inside a tank or the water resource.

The hardware is interfaced with all the sensors in the board. The hardware components include the microcontroller, relay, ADC converter, Virtuino app and all the sensors interfaced.

IV. ARCHITECTURE OF THE SYSTEM

4.1 Soil Moisture Sensor

A sensor that will sense the moisture level in the land (sand) called SOIL MOISTURE SENSOR.

4.2 Passive Infrared Sensor (PIR)

A PIR based motion detector is used to sense movement of people, animals or other objects

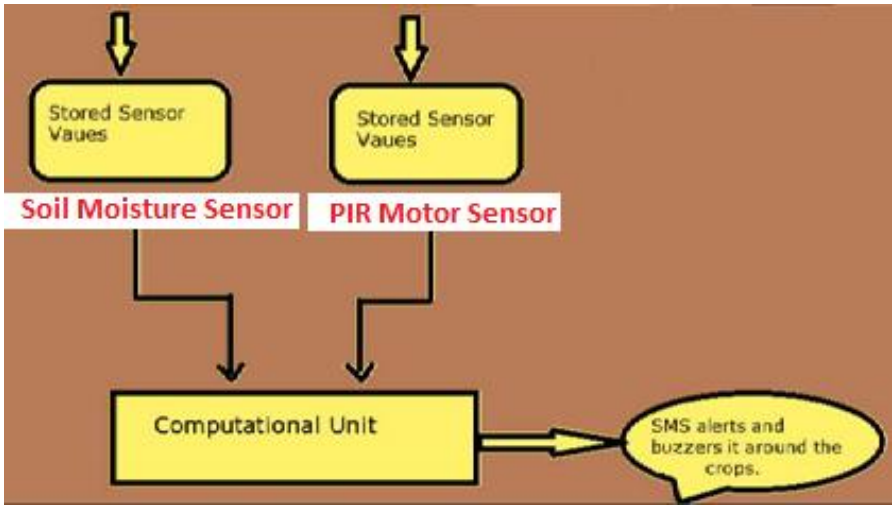

FIGURE 1: NODE1

Both SOIL MOISTURE SENSOR and PIR SENSOR are connected to the Arduino to perform an action. Arduino will send the data to the Thing speak server using wi-fi. If emergency it also send message and Alarm to the user by using Virtuino app.

V. EXPERIMENTATION AND RESULTS

As shown in figure 5, The sensors and microcontrollers of all Nodes are successfully interfaced with microcontroller and wireless communication is achieved between various Nodes.

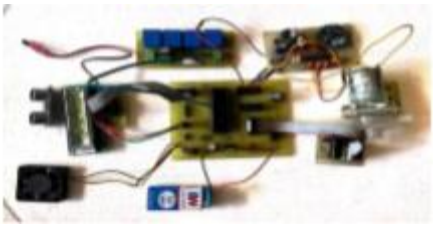

FIGURE 2: EXPERIMENTAL SETUP FOR NODE1

This is a complete solution to monitor garden activities and irrigation problems using sensors and microcontrollers respectively. Implementation of such a system in the garden can definitely help to improve the yield of the garden products and overall production.

VI. CONCLUSION

The sensors and microcontrollers of all Nodes are successfully interfaced with microcontroller and wireless communication is achieved between various Nodes.

All observations and experimental tests proves that propose project is a complete solution to kitchen garden /field activities, irrigation problems and pest management and control works respectively. Implementation of such a system in the kitchen garden can definitely help to improve the yield of the garden products and overall production.

REFERENCES

[1] Morais, Raul, A. Valente, and C. Serôdio. "A wireless sensor network for smart irrigation and environmental monitoring: A position article." In 5th European federation for information technology in agriculture, food and environement and 3rd world congress on computers in agriculture and natural resources (EFITA/WCCA), pp.45-850. 2005.

[2] K.Lakshmisudha, Swathi Hegde, Neha Kale, Shruti Iyer, " Smart Precision Based Agriculture Using Sensors", International Journal of Computer Applications (09758887), Volume 146-No.11, July 2011

[3] Nikesh Gondchawar, Dr. R.S.Kawitkar, "IoT Based Smart Agriculture", International Journal of Advanced Research in Computer and Communication Engineering (IJARCCE), Vol.5, Issue 6, June 2016.

[4] M.K.Gayatri, J.Jayasakthi, Dr.G.S.Anandhamala, "Providing Smart Agriculture Solutions to Farmers for Better Yielding Using IoT", IEEE International Conference on Technological Innovations in ICT for Agriculture and Rural Development (TIAR 2015).

[5] Chetan Dwarkani M, Ganesh Ram R, Jagannathan S, R. Priyatharshini, "Smart Farming System Using Sensors for Agricultural Task Automation", IEEE International Conference on Technological Innovations in ICT for Agriculture and Rural Development (TIAR 2015).

[6] S. R. Nandurkar, V. R. Thool, R. C. Thool, "Design and Development of Precision Agriculture System Using Wireless Sensor Network", IEEE International Conference on Automation, Control, Energy and Systems (ACES), 2014.

[7] Monika Jhuria, Ashwani Kumar, Rushikesh Borse, "Image Processing for Smart Farming: Detection of Disease and Fruit Grading", IEEE Second International Conference on Image Information Processing (ICIIP), 2013.

[8] Jhuria, Manoj, Ajit Kumar, and Rushikesh Borse. "Image processing for smart farming: Detection of disease and fruit grading." In Image Information Processing (ICIIP), 2013 IEEE Second International Conference on, pp.21-526. IEEE, 2013.

[9] González-Andújar, José Luis. "Expert system for pests, diseases and weeds identification in olive crops." Expert Systems with Applications 36, no. 2,pp 3278-3283 ,2009.

[10] Jim Chase: The Evolution of the Internet of Things. White Paper, Texas Instruments, September, 2013.

[11] Silvia, N. a. (2012). *International Food Prices.* ROME: FAO, IFAD,WFP.

[12] UN. (2012). *Kenya Food Security outlook.* Nairobi: kenya government.

[13] Pastakia, O. (2011). *livelihood Augementation in Rainfed Areas.* Gujarat, India: Development surport Centre(DSC).

[14] Denver Urban Gardens. (2012). *Denver Urban Gardens.* Retrieved December 15th, 2012, from Denver Urban Gardens: http://dug.org/gardens/

[15] Beddington, A. F. (2011). *Achieving Food Security In the Face of Climate Change.* Copenhagen: Commission on Sustainable Agriculture and Climate Change.

[16] Tittonell, G. (2012). *When yield Gaps are Poverty traps; The Paradigm of Ecological Intensification In Africa Smallholder Agiculture.*

[17] Mathai, R. J. (1985). *The Rural University: The Jawaja Experiment in Educational Innovation.* Popular Prakashan.

[18] Kimutai, E. K. (2012). *Bacteriological contamination of farm and market kale in Nairobi and Environs.* Nairobi

[19] Great Britain Ministry of Food. (1946). *How Britain was fed in war time: food control, 1939-1945.* London: Ministry of Food by H.M.S.O., 1946.

[20] Agobia. (1999). *Community Draught Mitigation Project,south African region.* Winnipeg: International Institute for Sustainable Development.

[21] Asaduzzaman, N. S. (2011). *Benefit-Cost Assessment of Different Vegetable Gardening on improving Household Foood and Nutritional Security in Rural Bangladesh.* Pittsburgh, Pensylvinia: Agricultural & Applied Economics Association's 2011 AAEA & NAREA.

50 m-range distance and position measurement method by using two searchlights for autonomous flight device

Hideki Toda[1], Kouhei Fujiuti[2]

Department of Electric and Electronic Engineering, University of Toyama, 3190 Gofuku, Toyama, 930-8555, Japan

***Abstract*—** *In the present study, 50 m-range distance and position measurement method for autonomous flight device such as four-rotor drone by using two searchlights was proposed, and the precise distance/position measurement performance was evaluated in an outdoor situation. To realize over 10 m long-distance flight of the drone under unstable GPS signal situations such as under the bridge or inside tunnels for periodic inspections, the correct self-position measurement is important for the stable control. This study is to propose a simple method of over 50 m range autonomous four-rotor helicopter movement control using high power 300W two searchlights as InfraRed sources on the ground and the direction of the searchlights sets to the investigation target position such as bridge side. High power light sources of the two searchlights are enabled to measure the correct drone position via an attached drone's camera with an InfraRed filter, and it realizes 1.5 m standard deviation position estimation error when 50 m distance in an outdoor daylight situation. In addition, the limitation of the position detectable condition also measured and analyzed in other experiments. Our proposed method would be effective in the situation that there is no skilled the drone control operator and the flight by visual confirmation of man are hard conditions, and useful to develop the position measurement system with low cost.*

***Keywords*— Four rotor helicopter, long distance / position measurement, InfraRed filter, two searchlights.**

I. INTRODUCTION

In this paper, 50 m-range distance and position measurement method for autonomous flight device such as four-rotor drone by using two searchlights was proposed, and the precise distance/position measurement performance was evaluated. Such as under the bridge, inside tunnels and buildings for the periodic inspection at unstable GPS signal situations, to realize over 10 m long-distance flight of the drone, since it is unable to confirm the real-time drone posture by the naked eye, easy and correct self-position measurement method is necessary for the stable inspection work [1,2] (Fig.1). Even if a human controls the drone, the flight by the naked eye of man is difficult in the over 10 m long distance flight [3-11], and another supporting mechanism of the position measurement and the control method would be necessary [12-25]. This study aims to propose a simple method of 50 m range distance and position measurement method for autonomous four-rotor helicopter using high power 100V AC two searchlights as InfraRed sources on the ground and evaluate the practical measurement ability of the distance/position in case of 50 m distance outdoor situation.

1.1 Previous study

Four-rotor helicopter does not include autonomous "position" controlling process as itself, and the positioning system is necessary to realize an inspection work [2]. To realize the position measurement, InfraRed 3D cameras or GPS sensor system generally have been used [9,14,26]. In the case of the InfraRed 3D camera, the precision of the position measurement is 1 mm order; however, the area of the using this method is within 10 m and the indoor situation only [5]. On the other hand, if the drone would be controlled in the outdoor situation, the GPS signal can be used that there are almost no obstacles upper direction (sky) and movement direction. However, to use the drone for the periodic inspection of under the bridge or inside tunnels, the two approaches could not be adopted since the instability of the GPS signal under the bridge or tunnel sites [2].

In our previous study [8], basic features of about 10 m area position measurement method using two searchlights had been proposed and analyzed, but the stability of the position measurement at a distance from 20 to 50 m with low reliability of the GPS signal was not discussed. This paper described the positional measurement performance of the proposed method until 50 m range, and the optical characteristics of each item of the camera, laser, searchlight with the geometric arrangement were summarized.

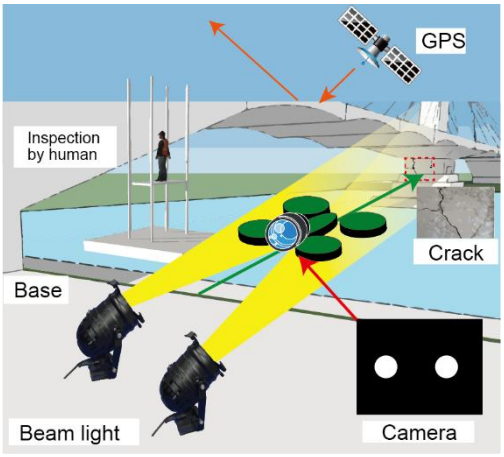

FIGURE 1. Proposed 50 m range distance/position measurement method using high power 100V AC two searchlights on the ground for autonomous four-rotor helicopter.

II. METHOD

Fig.2 illustrates an idea of the proposed method. High power two searchlights (Stage Evolution, PAR56SBG and SYLVANIA light, 0.16 m diameter light PAR56 300 W, SOUND HOUSE Corp.) were used for the InfraRed light sources on the ground. The camera (Ai-ball, QVGA 320x240 dots, 30 fps) at the front of the drone was tuned to the two searchlights direction, and it was controlled by using two searchlights positions on the camera image (using the center of gravity and the distance of the two points). There is an InfraRed filter (IR76,82,88, FUJI FILTER, FUJIFILM Corp.) in the front of the camera lens. The reason for using Ai-ball wireless camera is a considerable time delay of the drone's internal camera image transfer process, and control command transmitting (>around 100 msec). When the two bright spot positions are (x_1, y_1) and (x_2, y_2) on the camera image and the center of the gravity of the two points is $(G_x, G_y) = \left(\frac{x_1+x_2}{2}, \frac{y_1+y_2}{2}\right)$, the camera position (R_x, R_y) iscalculated as,

$$(R_x, R_y) = \left(\frac{G_x r}{\sqrt{(x_2-x_1)^2+(y_2-y_1)^2}}, \frac{\alpha r}{\sqrt{(x_2-x_1)^2+(y_2-y_1)^2}}\right) \quad (1)$$

where, the r is the distance between the searchlights and the α is the conversion factor between dot and real distance. The α is calculated when the distance between two searchlights and the camera was positioned 1 m apart and the camera is moved 1 m to the left or right. In this study, the α was calculated as 340.

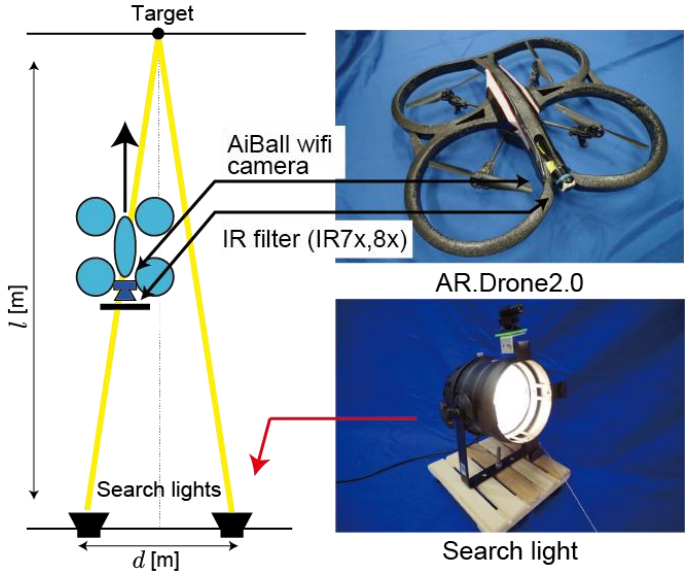

FIGURE 2. Basic concept of 50 m range position measurement method of the autonomous flight device. Two searchlights (Stage Evolution, PAR56BSG) were used for the position measurement of the drone in the space

III. EXPERIMENT

Experiment 1 confirmed the stability of drone's position measurement by measuring a camera image bright spot by changing the InfraRed filter in 10 m distance outdoor situation (Fig.3). This experiment reveals which wavelength of the InfraRed filter is effective in the experimental condition.

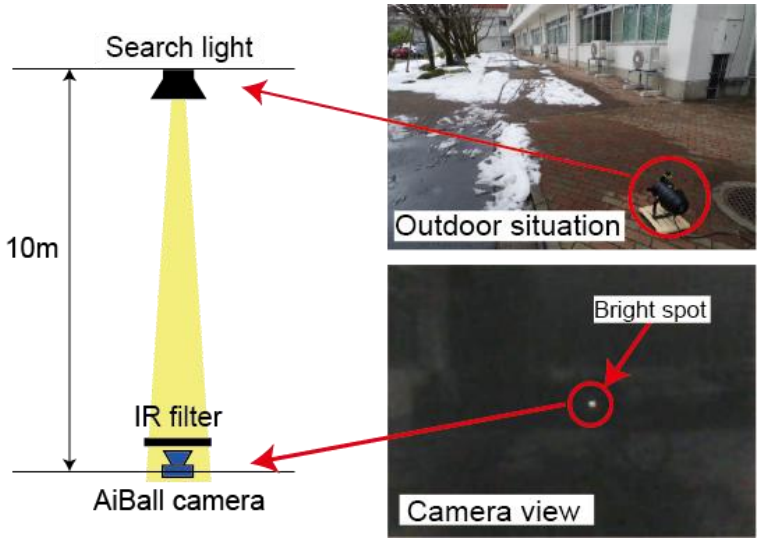

FIGURE 3. Experiment 1 setup of the 10 m distance bright spot measurement by Ai-ball camera at outdoor situation in case of IR76, 82, 88 InfraRed filter (passes wavelength below 760, 820, 880 nm respectively).

Experiment 2 measured the distance where the bright spots of the two searchlights do not merge in the camera image (Fig.4a). When the distance between the bright spots is less than six dots (almost all the cases, the area of each spot is about ten dots), the bright spots of the two searchlights are merged, and it is unstable to extract the two center of gravity points at the same time. This experiment reveals which distance the light of the searchlights reaches, and the drone (camera) can be measured.

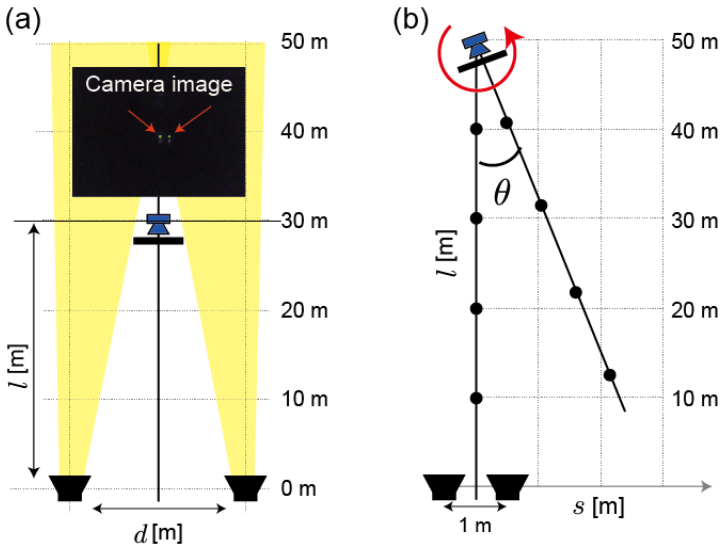

FIGURE 4. (a) Experiment 2 setup of the distance where the bright spots of the two searchlights do not merge in the camera image. (b) Experiment 3 setup of the distance by using the two spotlights when the angle of the camera was changed from 0 to 16 deg.

In the practical situation of the inspecting work by the drone, the angle of the camera on the drone would be fluctuated. Experiment 3 (Fig.4b) measured the distance by using the two spotlights when the angle of the camera was changed from 0 to 16 deg. In this experiment, the distance from the camera and the spotlights was changed from 10 to 50 m, and the distance of the two spotlights d sets as 1 m.

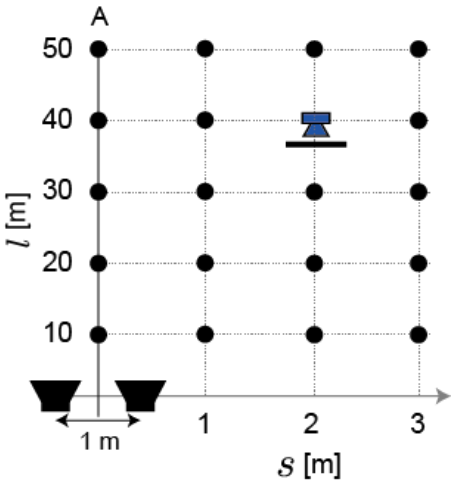

FIGURE 5. Experiment 4 setup of the 3 m×50 m range position / distance detectability measurement in outdoor situation.
The distance of the two searchlights was fixed as d=1 m.

In the last experiment 4, the practical position measurement accuracy in the outdoor environment was confirmed(Fig.5). Setup of the experiment was same with Fig.4a such that d=1 m, the distance between the camera and the searchlights takes l=10, 20, 30, 40, 50 m, and the distance from the center of two searchlights is changed s= 0, 1, 2, 3 m. It represents the total performance of the positional measurement accuracy of the proposed method.

IV. RESULT

Figure 6 represents the dependency of the InfraRed filter in 10 m distance outdoor situation. In Fig.6a, an example of the effect of the InfraRed filter was shown. The searchlight was positioned at (A), and it was extracted clearly by the IR filter (IR88 case). The dependency of the kind of IR filter was summarized in Fig.6b. Black solid bar and the error bar mean the average and the standard deviation of the brightness of the point (A) on the camera image. Without filter condition, the brightness takes a low value (avg. 55, maximum 255) and it was caused by the high brightness area such as snow via auto gain control mechanism of the camera. On the other hand, with IR filter condition, the brightness of the point (A) take over 200 with low error. Fig. 6c means the brightness of the point (B), it was white colored snow area. In without filter condition, even though the brightness takes over 200 (it was white), the brightness of the point (B) with IR filter was reducing with increasing of the wavelength. As the conclusion, the IR88 filter represents a good performance compared with other filters. After this experiment, the IR88 filter was used in below experiments.

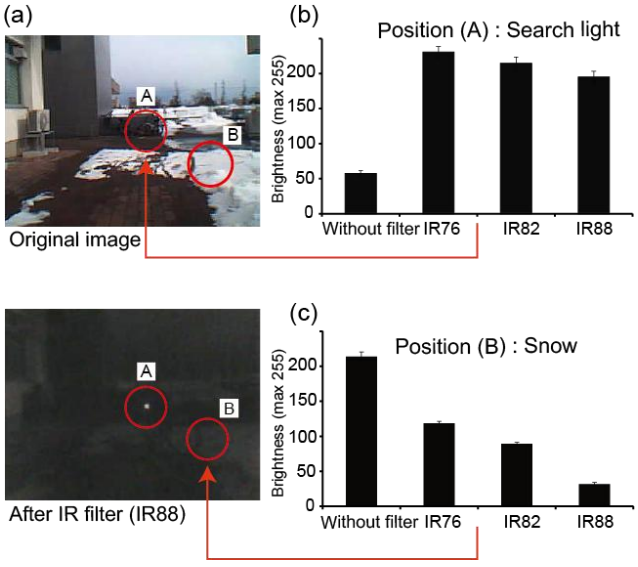

FIGURE 6. Result of the dependency of the InfraRed filter (IR76, IR82, IR88). (a) Original image and after IR filter image. (b) The brightness measurement result of thesearchlight position (N=5). (c) The brightness measurement of the snow area (other area of the searchlight).

Figure 7 represents the result of the distance where the bright spots of the two searchlights do not merge in the camera image (experiment 2). Black circle dot means the spotlights distance d when the distance between two bright spots was seven dots in the camera image. For example, to detect the position/distance around 50 m, it is necessary to set d=0.75 m or above as the searchlights distance d. The black circle dots show the minimum distance d of the two searchlights in each distance l from 10 to 50 m, and the linear approximation was calculated as $d = 0.017l$ ($R^2 = 0.999$). It means that when the position/distance measurement was needed around l m, the distance between two searchlights d is necessary above $d = 0.017l$ (green area of Fig.7).

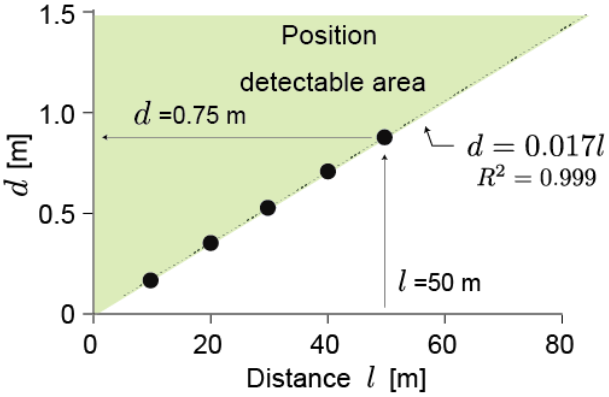

FIGURE 7. Result of the limitation of the distance / position measurement (experiment 2). Black dots mean that the distance between two searchlights equals to 7 dots in the camera image when the distance l is changed from 10 to 50 m.

Figure 8 shows the result of the camera angle dependency where the l=10, 20, 30, 40, 50 m, and the camera angle was changed from 0 to 16 deg. The plots mean the estimated positions (s, l) from the camera image analysis, and dotted circles are the ideal positions. As shown in small black arrows, the positional shift from the ideal position was increased with the camera angle. For example, the estimated distance l was 46.7 m (S.D. is 0.59 m, N=5 times experiment) in the case of camera angle 16 deg when ideal distance was l=50 m. The displacement was 50-46.7=2.8 m in this case. On the other hand, if the displacement would be suppressed within 1 m when 50 m distance (that means 50-1=49 m), since the approximation equation was calculated as $l = -0.212\theta + 50.23 (R^2 = 0.96)$ from Fig.8, it is necessary to limit the camera angle within $\theta = (49 - 50.23)/-0.212$=5.8 deg as one side (right or left).

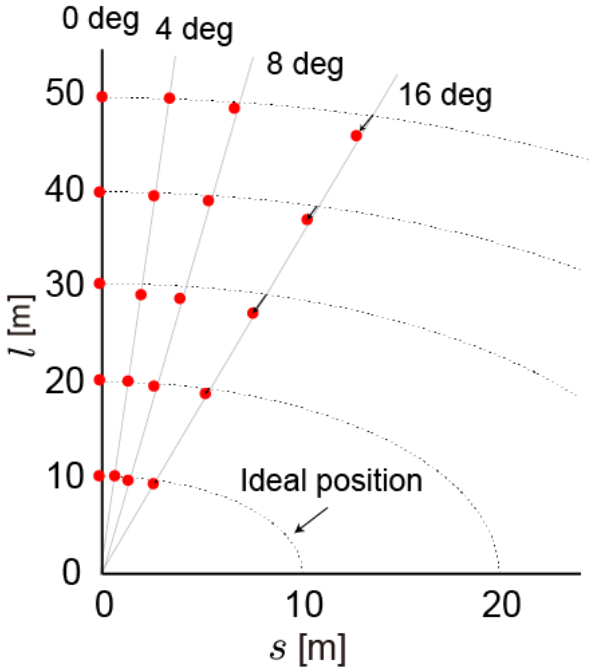

FIGURE 8. Result of the position estimation displacement when the camera angle was changed from 0 to 16 deg (experiment 3). The dotted lines mean the ideal position if there are no errors by changing the camera angle

In Fig.9, the practical position measurement accuracy in the outdoor environment by the proposed method was summarized (N=5). The blue dots and the error bar of l and s axis shows the average and the standard deviation. S.D. takes small value in the small range of l, and there was (s, l)=$(3.1 \pm 0.08, 52.1 \pm 1.5)$ m (avg.±S.D.) in the point of B (correctly, the position is $(s, l) = (3{,}50)$ m). Since the error rates of each axis were calculated as $0.08/3.1$=2.58% of s axis and $1.5/52.1$=2.88% of l, there are about 3% errors in the position measurement process in l=50m point. Above result would be useful for unstable GPS situation such as under the bridge, inside tunnels and buildings for the periodic inspection to realize easy setup and low cost 50 m range position/distance measurement method.

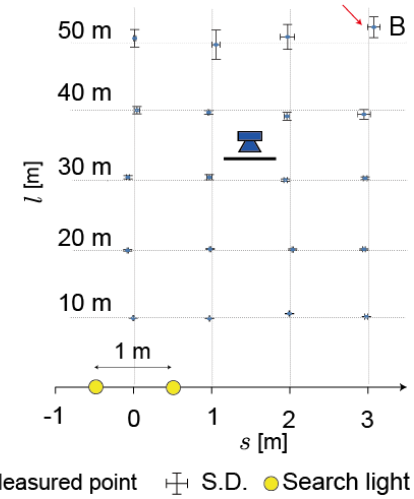

FIGURE 9. Result of the 3 m× 50 m area position estimation performance (experiment 4). Blue dots represent the average estimated position from the two searchlights position on the camera image (N=5 times experiment average). Error bars show the S.D. of the measurement.

V. DISCUSSION

In our previous study [8], the four-rotor drone (using AR Drone model helicopter) was controlled and flighted by the two searchlights system from 5 to 10 m distance area. However, the position control of the drone was unstable especially when the long-distance flight over 10 m. In the study [8], the unstable reason could not be cleared, and it would be concluded as there are two factors (1) the drone position control theory itself, (2) the position measurement method. This study aims to clear the effect of the position measurement method using the two searchlights.

One of the general solutions of the position measurement is to use a large area colored marker board, however, by attaching the large area red marker board would cause the wind flow instability and could not acceptable especially in the far distance inspection sites such as bridges or tunnels. The advantage of the proposed method would be easy to find the searchlight points by using the InfraRed regions, and it would realize the correct 50 m range position measurement just by attaching a small wireless camera on the drone. In our experiment, the resolution of the attached camera was low resolution 320×240, but it could be realized more precise position measurement by using a high-resolution camera.

VI. CONCLUSION

In this paper, 50 m-range distance and position measurement method for autonomous flight device such as four-rotor drone by using two searchlights was proposed, and the precise distance/position measurement performance was evaluated in an outdoor situation. This study is to propose a simple method of 50 m range distance / position measurement using high power 300 W two searchlights as InfraRed sources on the ground. In experiment 1, the IR88 (wavelength is 880 nm) InfraRed filter extracts only the light of the searchlights and it is not affected by ambient light such as light reflected on the white snow. Experiment 2 measured the maximum distance/position detectable area of the drone (camera position), and it was affected by the d of the distance between two searchlights (the l and d take a linear approximation relationship $d = 0.017l$ at least 50 m). The result of experiment 3 shows the distance/position displacement by the camera angle changes from 0 to 16 deg, and the displacement was extended by increasing of the camera angle θ, and there was 2.8 m displacement when 50 m distance and 16 deg condition. In the last experiment 4, the positional measurement accuracy in the area of 3 m × 50 m was confirmed when d=1 m condition. There were about 3% displacement errors in each axis s and l, and this evaluation results would be useful to develop the position measurement system with low cost.

REFERENCES

[1] K.Nonami, F.Kendoul, S.Suzuki, W.Wang, and D.Nakazawa, "Autonomous flying robots : unmanned aerial vehicles and micro aerial vehicles, "Springer Japan, 2010.

[2] Ministry of Land (Japan), Infrastructure and Transport, bridge maintenance Subcommittee, Liang maintenance technology site verification and evaluation of the results, March 19, 2015.

[3] E. Altug, J.P. Ostrowski, and C.J. Taylor, "Control of a quadrotor helicopter using dual camera visual feedback," International Journal of Robotics Research, vol.24, no.5, 2005, pp.329-341.

[4] B. Ludington, E.Johnson, and G.Vachtservanos, "Augmenting UAV autonomy: vision-based navigation and target tracking for unmanned aerial vehicles," IEEE Robotics and Automation Magazine, vol.13, no.3, 2006, pp.63-71.

[5] H. Takano andH. Toda, "Roll movement realized by yaw and roll command combination method of AR Drone 4 rotor helicopter for improving stability of automatic position stop," International Conference on Advanced Mechatronics (ICAM 2015), Waseda University, Tokyo, Japan, Dec.5-8, 2015, p. 53.

[6] H. Toda, H. Syuichi, and H. Takano, "Effectiveness of Fast Speed Yaw and Roll Control Switching Instead of Normal Roll Control for AR Drone 4 rotor Helicopter," International Journal of Innovative Research in Advanced Engineering, vol. 3, issue 7, Paper ID JYAE10081, doi:10.17632/y52bmbgtkg.1, July 2016.

[7] H. Toda and H. Takano, "Effect of Discrete Yaw Direction Setting for 4 Roter Helicopter Control: Computer Simulation and AR. Drone Model Implementation," International Journal of Innovative Research in Advanced Engineering, vol. 3, issue 7, Paper ID JYAE10086, doi:10.17632/cj8f3v6csr.1, July 2016.

[8] H. Toda and K.Fujiuti, "Experimental Study on 4 Rotor Helicopter 10m-Range Distance and Position Measurement Method by Using Two Searchlights for Autonomous Control and the Evaluation," International Journal of Robotics and Automation Technology, vol. 3, 2016.

[9] S. Azrad, F. Kendoul, and K. Nonami, "Visual Servoing of Quadrotor Micro-Air Vehicle Using Color-Based Tracking Algorithm," Journal of System Design and Dynamics (JSME), vol. 4, no. 2, 2010, pp. 255-268.

[10] B. Ludington, E. Johnson, and G.Vachtservanos, "Augmenting UAV autonomy: vision-based navigation and target tracking for unmanned aerial vehicles," IEEE Robotics and Automation Magazine, vol.13, no.3, 2006, pp.63-71.

[11] K. Nonami, "Rotary Wing Aerial Robotics," Journal of Robotics Society of Japan, vol. 24(8), 2006-11-15, pp. 890-896.

[12] J. Engel, J. Sturm, and D. Cremers, "Camera-based navigation of a low-cost quadrocopter,"IEEE/RSJ, Intelligent Robots and Systems (IROS), 2012.

[13] R. Mahony and T. Hamel, "Image-based visual servo control of aerial robotic systems using linear image features," IEEE Trans. on Robotics, vol.21, issue 2, pp.227-239, 2005.

[14] Y. Kubota and T. Iwatani, "Dependable visual servoing of a small-scale helicopter with a wireless camera," Proceedings of the 2011 Conference on Robotics and Mechatronics, 1A2-O15, Okayama, Japan, May 26-28, 2011.

[15] T.K. Roy, M. Garratt, H.R. Pota, and M.K. Samal, "Robust altitude control for a small helicopter by considering the ground effect compensation," Intelligent Control and Automation (WCICA), 2012 10th World Congress, DOI:10.1109/WCICA.2012.6358168, 2010, pp.1796-1800.

[16] O. Andrisani, E.T. Kim, J. Schierman, and F.P. Kuhl, "A nonlinear helicopter tracker using attitude measurements, "IEEE Transactions on Aerospace and Electronic Systems, vol. 27, issue 1, DOI:10.1109/7.68146, 1991, pp.40-47.

[17] F. Chen, B. Jiang, and F. Lu, "Direct adaptive control of a four-rotor helicopter using disturbance observer, "International Joint Conference on Neural Networks (IJCNN), 2014, pp.3821-3825.

[18] A.C. Satici, H. Poonawala, and M.W. Spong, "Robust Optimal Control of Quadrotor UAVs,"IEEE Access, vol.1, DOI:10.1109/ACCESS.2013.2260794, 2013, pp.79-93.

[19] J. Toledo, L. Acosta, M. Sigut, and J. Felipe, "Stability Analisys of a Four Rotor Helicopter," Automation Congress, WAC '06. World, 2006, pp.1-6.

[20] P. Castillo, A. Dzul, and R. Lozano, "Real-time stabilization and tracking of a four-rotor mini rotorcraft", IEEE Transactions on Control Systems Technology, vol. 12, issue 4, DOI:10.1109/TCST.2004.825052, 2004,pp.510-516.

[21] O. Meister, N. Frietsch, C. Ascher, and G. F. Trommer, "Adaptive path planning for a VTOL-UAV," Position, Location and Navigation Symposium, 2008 IEEE/ION, DOI:10.1109/PLANS.2008.4570046, 2008, pp. 1252-1259.

[22] L. Garcia-Delgado, A. Dzul, V. Santib, and M. Llama, "Quad-rotors formation based on potential functions with obstacle avoidance," Control Theory and Applications, IET, vol. 6, issue 12, DOI:10.1049/iet-cta.2011.0370, 2012, pp.1787-1802.

[23] F. Kendoul, Z. Yu, and K. Nonami, "Embedded autopilot for accurate waypoint navigation and trajectory tracking: Application to miniature rotorcraft UAVs," Robotics and Automation, 2009 ICRA '09. IEEE International Conference on, DOI:10.1109/ROBOT.2009.5152549, 2009, pp.2884-2890.

[24] (2016) K. Nomura, "Industrial applications type electric multi-rotor helicopter, introduction of mini-surveyor and flight demonstration," Mini-surveyor consortium, [Online], Available on :http://mec2.tm.chiba-u.jp/~nonami/consortium/outline.html/

[25] E. Altu, J. P. Ostrowski, and R. Mahony, "Control of a Quadrotor Helicopter Using Visual Feedback," Proceedings of the 2002 IEEE International Conference on Robotics and Automation, Washington DC, May 2002.

[26] K. Watanabe, Y. Iwatani, N. Kenichiro, and K. Hashimoto, "A vision-based support system for micro helicopter control," Proceedings of the 2008 Conference on Robotics and Mechatronics, 1P1-F13, Nagano, Japan, June 5-7, 2008.

AD Publications
Sector-3, MP Nagar, Bikaner,
Rajasthan, India
www.adpublications.org, info@adpublications.org